IV. TRABAJO 2.

The Unfolding Pathway of Leech Carboxypeptidase Inhibitor

IV.A. INTRODUCTION

Leech carboxypeptidase inhibitor (LCI) is the first metallocarboxypeptidase inhibitor found in leeches *(1).* LCI is a cysteine-rich polypeptide of 66 residues that behaves as a tight binding and competitive inhibitor of different types of pancreatic-like carboxypeptidases (A1, A2, B, and plasma carboxypeptidase B) with equilibrium dissociation constants K_i of 0.1-0.4 × 109 M *(1).* The lowest K_i value of LCI is shown for plasma carboxypeptidase B, an enzyme also known as thrombin activable fibrinolysis inhibitor (TAFI), that proteolytically removes C-terminal residues from fibrin and down-regulates plasminogen activation, leading to an attenuation of fibrinolysis *(2, 3).* Assuming that the leech secretes LCI during feeding, this inhibitor may help to maintain blood in the fluid state. The profibrinolytic effect of LCI has recently been demonstrated in an in vitro system, suggesting a potential application to human therapy. In this regard knowledge of the stability and folding behavior of LCI constitutes a basis for the development of variants of the molecule with enhanced activity and/or stability. The recently published three-dimensional structure of LCI shows that it folds in a compact domain consisting of a five-stranded antiparallel β-sheet and a short α-helix *(4).* One of the main contributions to the stability of native LCI arises from the occurrence of four disulfide bridges between cysteines 11-34, 18-62, 19-43, and 22-58, all of them located within regular secondary structure elements. The unstructured C-terminal tail of LCI interacts with the carboxypeptidase in a substrate-like manner, similar to what was previously described for the potato carboxypeptidase inhibitor (PCI). No sequential homology is observed between PCI and LCI except for the C-terminal tail; however, both proteins show the structural feature of being stabilized by disulfide bridges.

For disulfide-containing proteins, unfolding and refolding generally correlate with reduction and oxidation of the native disulfides *(5, 6).* Since the intermediates generated in these processes can chemically be trapped and characterized, it is possible to derive in detail the disulfide unfolding and refolding pathways. We have recently described a new methodology to determine stability toward denaturants and to elucidate the unfolding pathway of disulfide-containing proteins *(7, 8).* This approach is based on the observation that the presence of trace amounts of a thiol initiator during unfolding by denaturants generates a mixture of scrambled species mostly consisting of non-native disulfides that still maintain the native number of disulfide bonds. This method has been applied to characterize the unfolding pathway of several disulfide-containing proteins, namely tick anticoagulant peptide (TAP) (3 disulfides) *(8),* PCI (3 disulfides) *(9),* and insulin-growth factor (IGF-1) (3 disulfides) *(10).*

In the present work we describe the unfolding pathway and conformational stability of LCI derived from the characterization of the scrambled species generated in the presence of a thiol initiator. The comparison to other disulfide-containing proteins offers an insight into the role of disulfide bonds in guiding the folding pathway and stabilizing the native fold.

IV.B. EXPERIMENTAL PROCEDURES

IV.B.1. Materials.

Recombinant LCI was obtained by heterologous expression in Escherichia coli following a procedure previously described *(1).* The recombinant protein that contains a construction-added glycine as the N-terminal residue was purified by ion-exchange chromatography on a TSK DEAE column (Amersham Biosciences) followed by reverse-phase HPLC. The protein was over 99% pure, as judged by HPLC, and its molecular mass was confirmed by MALDI-TOF. Urea, guanidine hydrochloride (GdnHCl), guanidine thiocyanate (GdnSCN), and acetonitrile with purities greater than 99%, were obtained from Merck (Darmstadt, Germany).

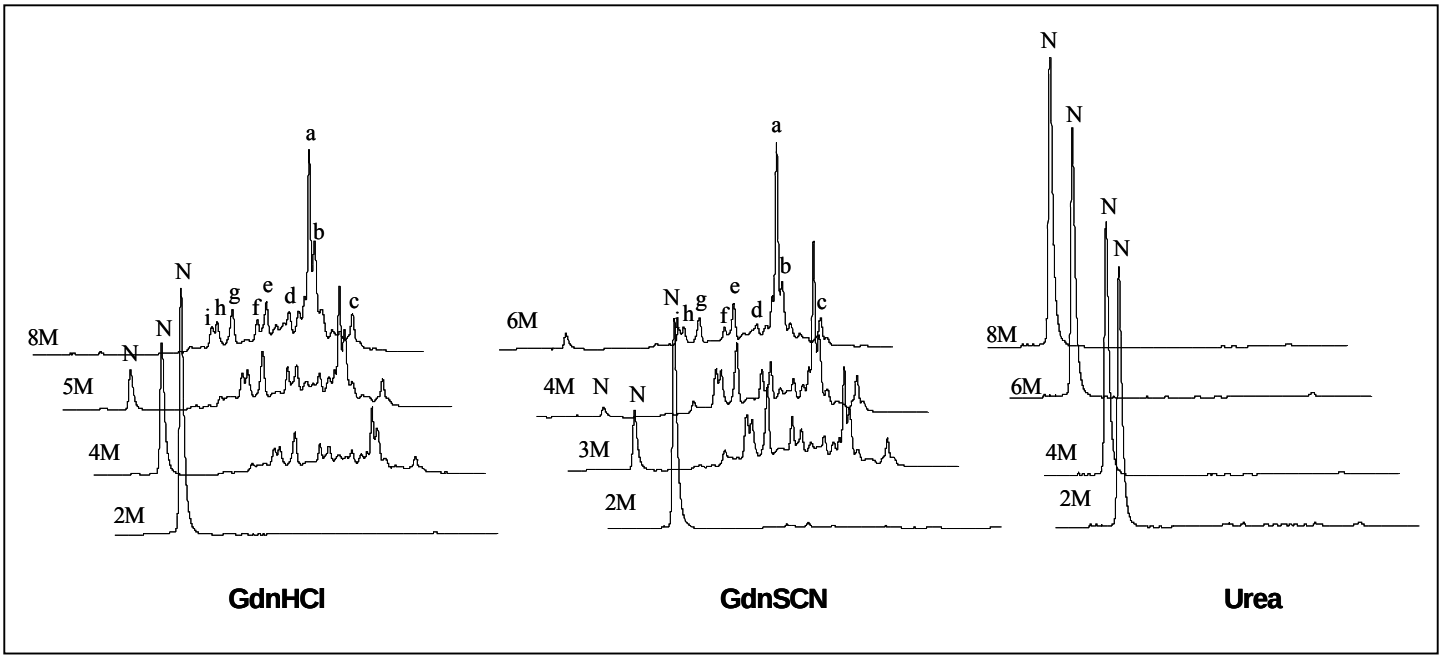

Figure 1. Denatured states of LCI under different concentrations of urea, GdnHCl, and GdnSCN. Native LCI was denatured in Tris-HCl buffer (0.1 M, pH 8.4) containing 2-mercaptoethanol (0.25 mM) and the indicated concentrations of the denaturant at 20 °C for 20 h. The denatured sample was quenched with equal volumes of 4% aqueous trifluoroacetic acid and analyzed by HPLC. The solvents used were: solvent A, 0.1% trifluoroacetic acid in water; solvent B, acetonitrile/water (9:1, v/v) containing 0.085% trifluoroacetic acid. The sample was applied to a Zorbax 300SB C-18 column (4.6 mm × 5 μm), and a linear gradient was developed between 31 and 47% of solvent B in 45 min. Column temperature was 23 °C. N indicates the elution position of the native species. Scrambled four-disulfide species are marked alphabetically (a-i).

IV.B.2. Denaturation and Unfolding of LCI in the Presence of a Thiol Initiator.

Native LCI (0.5 mg/ml) was dissolved in Tris-HCl buffer (0.1 M, pH 8.4) containing 0.25 mM 2-mercaptoethanol and selected concentrations of denaturants (urea, GdnHCl, GdnSCN, or organic solvent). The reaction was allowed to reach equilibrium and was typically performed at 23 °C for 20 h *(8)*. To monitor the kinetics of unfolding, aliquots of the sample treated with selected concentrations of GdnHCl were removed at time intervals, quenched with an equal volume of 4% aqueous trifluoroacetic acid, and directly analyzed by HPLC or kept at 20 °C until analysis. The GdnSCN-denatured samples were further purified by gel-filtration (NAP-5 columns from Amersham Biosciences) and eluted with 1% trifluoroacetic acid prior to HPLC analysis. To follow the time course of LCI unfolding, native LCI was dissolved in the same buffer containing 6, 7, or 8 M GdnHCl. At given incubation times, aliquots were removed, quenched with an equal volume of 4% trifluoroacetic acid, and analyzed by HPLC. Heat denaturation was performed by submitting aliquots of the sample in Tris-HCl buffer (0.1 M, pH 8.4) containing 0.25 mM 2-mercaptoethanol to increasing temperatures of 45, 55, and 65 °C for 1 h and finally quenching the sample with equal volumes of 4% trifluoroacetic acid.

IV.B.3. Fluorescence Spectra of Urea and GdnHCl-Treated LCI.

The fluorescence spectra of LCI were measured with a 650-40 spectrofluorometer (PerkinElmer) scanning from 300 to 450 nm with excitation at 280 nm. LCI was dissolved in Tris-HCl buffer (0.1 M, pH 8.4) containing 0.25 mM 2-mercaptoethanol and selected concentrations of denaturants (urea and GdnHCl). Denaturation of LCI was performed at 23 °C for 20 h. The final concentration of LCI was 2 µM. Fluorescence intensities of blank samples containing equivalent concentrations of the denaturant were also analyzed and subtracted from readings of the LCI samples.

IV.B.4. Structural Analysis of Scrambled LCI.

Isolated fractions of scrambled LCI (20 µg) were treated with 2 µg of thermolysin (Sigma, P-1512) in 30 µl of N-ethylmorpholine/acetate buffer (50 mM, pH 6.4). Digestions were carried out for 16 h at 37 °C for species X-LCI-g and at 50 °C for X-LCI-a. The reaction products were then fractionated by HPLC and analyzed by amino acid sequencing and mass spectrometry to identify the disulfide-containing peptides.

IV.B.5. Amino Acid Sequencing and Mass Spectrometry.

The amino acid sequence of disulfide-containing peptides was analyzed by automated Edman degradation using a PerkinElmer Procise sequencer (model 494) equipped with an on-line phenylthiohydantoin-derivate analyzer. The molecular mass of disulfide-containing peptides was determined by MALDI-TOF mass spectrometry (Bruker Biflex TOF spectrometer equipped with a nitrogen laser with an emission wavelength of 337 nm).

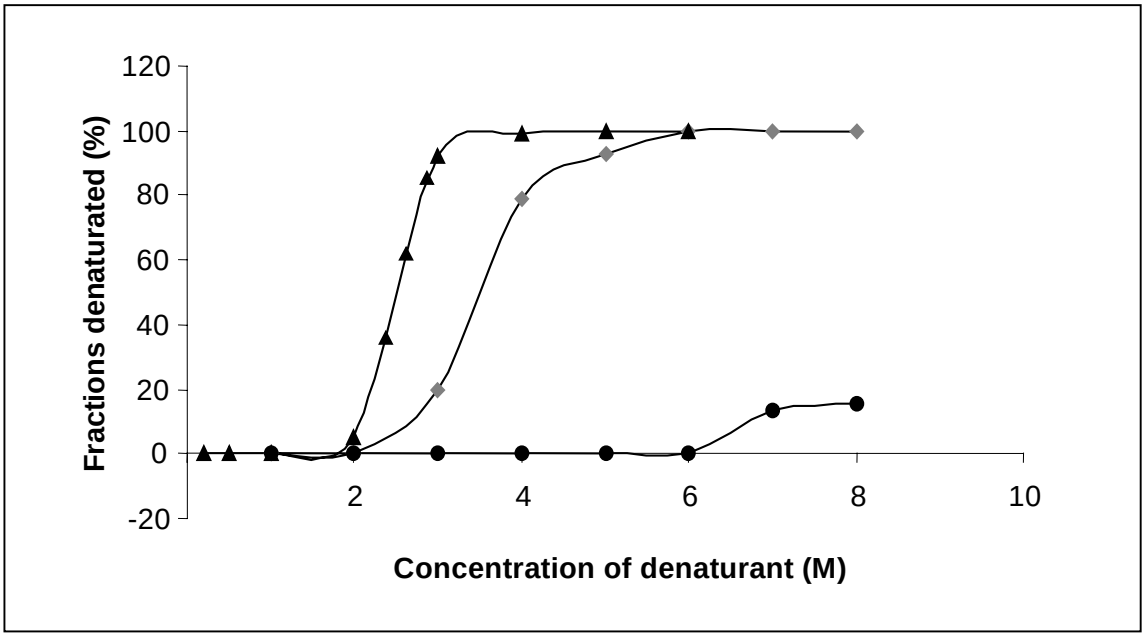

Figure 2. LCI denaturation curves. The denatured fraction is expressed as the percentage of LCI that is converted to scrambled isomers. The denaturants are GdnSCN (◆), GdnHCl (▲), and urea (●). Denaturation was carried out at 20 °C for 20 h in Tris-HCl buffer (0.1 M, pH 8.4) containing 2-mercaptoethanol (0.25 mM) and the indicated concentrations of denaturant.

IV.B.6. Plotting of the Denaturation and Unfolding Curves of LCI.

Denaturation of native LCI is defined by the conversion of the native structure to scrambled isomers. The denaturation curve was therefore generated by plotting the percentage of native LCI converted to scrambled isomers under increasing concentrations of a selected denaturant. In contrast, unfolding describes the state of the denatured LCI and is structurally defined by the composition of scrambled isomers. The LCI unfolding curves are determined by the relative concentrations of different scrambled isomers that exist along the unfolding pathway under increasing concentrations of a selected denaturant. Calculation of the yield of scrambled isomers was based on peak area integration. The data shown have a S. D. of ±5%.

IV.C. RESULTS

IV.C.1. Denaturation and Unfolding of the Native LCI in the Presence of Urea, GdnHCl, and GdnSCN.

Native LCI was allowed to denature and unfold to form scrambled isomers in the presence of a thiol initiator and increasing concentrations of urea, GdnHCl, and GdnSCN. The HPLC profiles of the different states of unfolding are displayed in Fig. 1. Though it is not possible to determine how many scrambled isomers of LCI of the 104 possible ones populate the unfolded state, 9 of them, which amount to 90% of total denatured LCI, can be distinguished. They appear marked alphabetically in Fig. 1 (a-i). The denaturation curves, calculated from the percentage of LCI converted to scrambled isomers, are shown in Fig. 2. Unfolding of LCI cooperatively occurs at 2-3 M GdnSCN with a midpoint at 2.4 M and at 3-4 M GdnHCl with a midpoint at 3.6 M. Based on the concentration that is required to achieve the same extent of denaturation, GdnSCN is about 1.5-fold more potent than GdnHCl. In contrast, urea is unable to denature the native LCI, because even at high concentration (8 M) the scrambled species are undetectable. Although urea is normally expected to be a weaker denaturant than GdnHCl *(11),* LCI represents an extreme case in resistance to urea denaturation because even PCI, one of the more stable of the disulfide-containing proteins studied so far against urea denaturation, is about 50% denatured in 8 M urea *(9).*

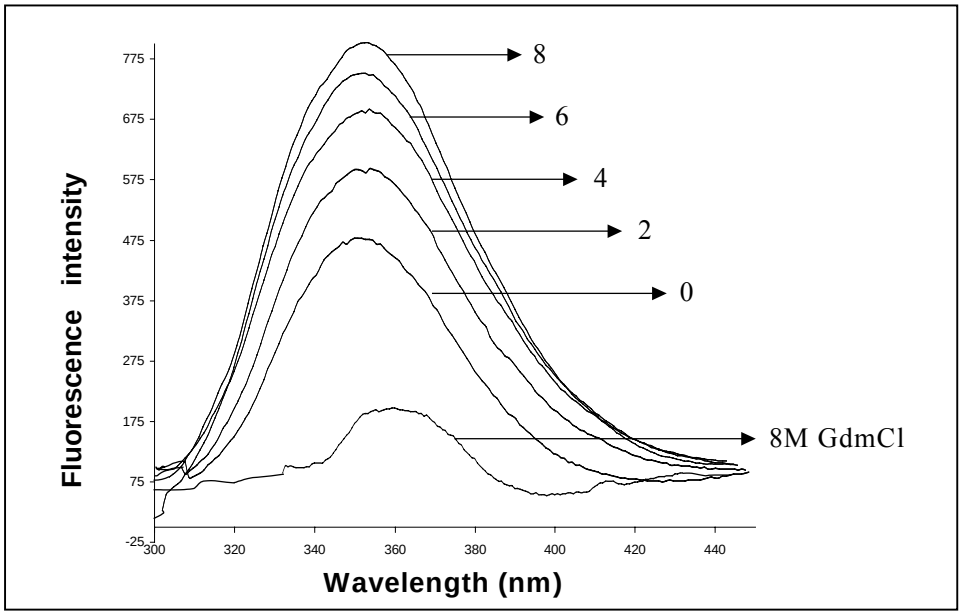

Figure 3. The fluorescence spectra of urea-treated LCI. Excitation wavelength was set at 280 nm, and protein concentration was 2 μM. Numbers associated with arrows indicate molar concentration of urea. The number 0 indicates the spectrum of native LCI. The spectrum of LCI denatured in the presence of 8 M GdnHCl was taken as the fully denatured LCI.

IV.C.2. Fluorescence Spectra of Urea and GdnHCl-treated LCI.

Given the previous results obtained with the urea treatment and to ensure that no scrambled species hypothetically generated could have remained undetected, the behavior of the molecule upon urea and GdnHCl treatment was followed by fluorescence measurements. LCI contains two tryptophan residues at sequence positions 42 and 50. LCI exhibits increased fluorescence intensities when treated with increasing urea concentrations, albeit without any concomitant redshift. In contrast, treatment with 8 M GdnHCl generates a spectrum with decreased intensity and a clear redshift from 354 to 360 nm (Fig. 3). Since a displacement of the maximum of fluorescence, rather than a change in intensity, indicates denaturation, this observation supports the previously drawn conclusion that urea is unable to denature LCI.

IV.C.3. Denaturation of LCI in Organic Solvents and Heat Denaturation of LCI.

LCI was treated with increasing concentrations of methanol, allowing the reaction to reach equilibrium in 48 h. No denaturation at all was observed even at 65% methanol (data not shown). The same result was found when applying a standard heat denaturation procedure. Even at 65 °C with an incubation time of 1 h, no conversion of native LCI into denatured species was observed, supporting a previous observation of resonances related to the presence of three-dimensional structure by NMR at high temperatures *(1).*

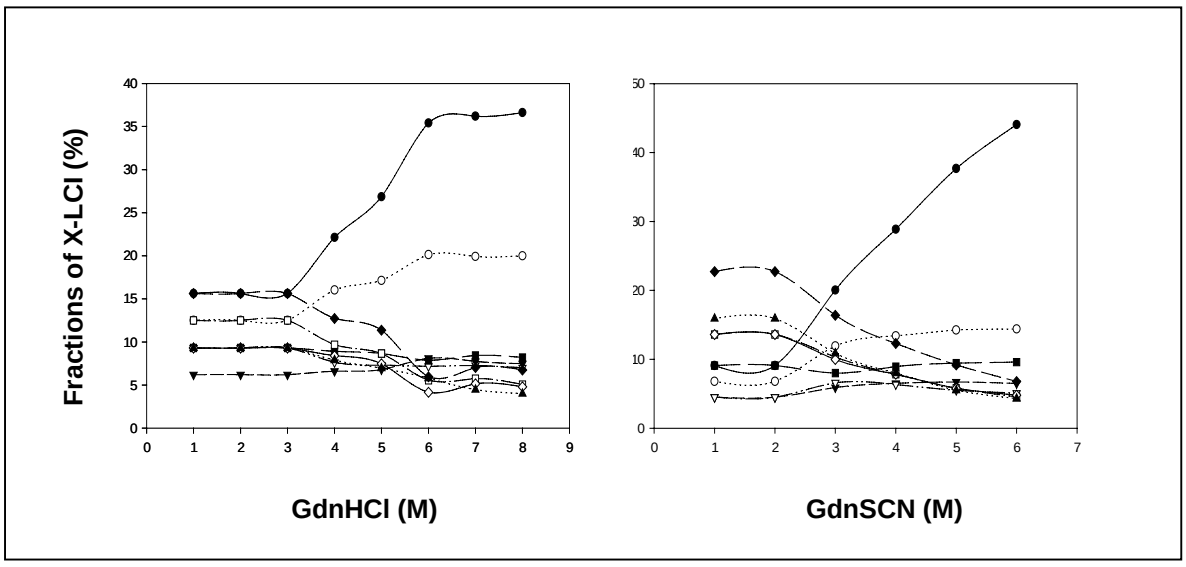

Figure 4. The unfolding curves (pathways) of LCI. The recoveries of six scrambled isomers of the denatured LCI are plotted against concentrations of two denaturants, GdnHCl and GdnSCN. X listed below refers to scrambled, and a-g refers to fractions thus identified in Fig. 1. X-LCI-a (●), X-LCI-b (❍), X-LCI-c (▼), X-LCI-d(∇), X-LCI-e (■), X-LCI-f (❑), X-LCI-g (◆), X-LCI-h (◊), X-LCI-i (▲). S.D. (not shown) is ±5%.

IV.C.4. The Unfolding Curve (Pathway) of LCI.

The pathway of LCI unfolding can be represented by plotting the relative concentrations of the scrambled isoforms of denatured LCI along the process. The data corresponding to the evolution of the nine scrambled LCI isomers in the presence of increasing concentrations of GdnHCl and GdnSCN are shown in Fig. 4. Because of the almost complete inability of urea to unfold LCI, the unfolding curves are not shown for this condition. The relative concentrations of X-LCI-a and X-LCI-b correlate with the strength of the denaturing conditions in both cases. This phenomenon is more easily observed in GdnSCN curves where an increase in the relative concentration of X-LCI-a from 10 to 45% is observed within the interval of 2-6 M GdnSCN, while an increase from 15 to 37% is observed within the interval of 3-6 M GdnHCl. To a lower extent X-LCI-b shows the same phenomenon. X-LCI-f, X-LCI-g, and X-LCI-h show an inverse correlation between their relative abundances and the denaturing conditions. X-LCI-g shows the biggest differences (25-26% in a range of 1-6 M GdnSCN). Among these three species, X-LCI-g is the most highly populated scrambled at low concentrations of GdnHCl (16%) and GdnSCN (25%). X-LCI-g is followed by X-LCI-f and X-LCI-h (both 14% in GdnSCN and 12 and 8% in GdnHCl, respectively). According to these results, it is possible to separate the scrambled isomers of LCI into two groups, which suffer a different kind of evolution along the unfolding pathway. Two species, X-LCI-a and X-LCI-g, which represent each population and show the higher relative concentration at extremes of denaturant concentration, were selected to further study their disulfide pairing and be structurally characterized.

IV.C.5. The Disulfide Structures of Scrambled Isomers of LCI.

Along the unfolding pathway of LCI, 9 major fractions can be identified as scrambled isomers, distinguishable from a population of 104 possible isoforms (Fig. 1). They were separated by reverse-phase HPLC with a linear acetonitrile gradient. Two fractions, X-LCI-a and X-LCI-g, selected according to the aforementioned criteria, were further isolated and analyzed to determine their disulfide structures. After digestion with thermolysin, peptides were isolated by HPLC and characterized by Edman sequencing and mass spectrometry to identify the disulfide pairing. Table I summarizes the sequence and mass spectrometry analyses of the peptides isolated after digestion of the two scrambled isomers.

X-LCI-a was clearly identified as the beads-form isomer (contains Cys11-Cys18, Cys19-Cys22, Cys34-Cys43, and Cys58-Cys62 bonds) (Fig. 5) from the unambiguous results summarized in Table I. The structure of X-LCI-a was deduced from the identification of three

major thermolytic peptides, a-4, a-10, and a-9, that showed an unique possible Cys pairing (Table I) consistent with sequencing and mass spectrometry.

X-LCI-g adopts Cys11-Cys62, Cys18-Cys22, Cys19-Cys34, and Cys43-Cys58 pairing (Fig. 5). From the unambiguous analysis of peptide g-11, and according to its determined Mr (2426.39), Cys43-Cys58 was the first disulfide pair assigned. The analysis of g-5 showed two separated sequences bound by a unique disulfide pair, Cys19-Cys34. Both disulfide pairs helped to further define the pairing of peptides g-8 and g-9, whereas only one disulfide pair could fit out of a mixture of possibilities.

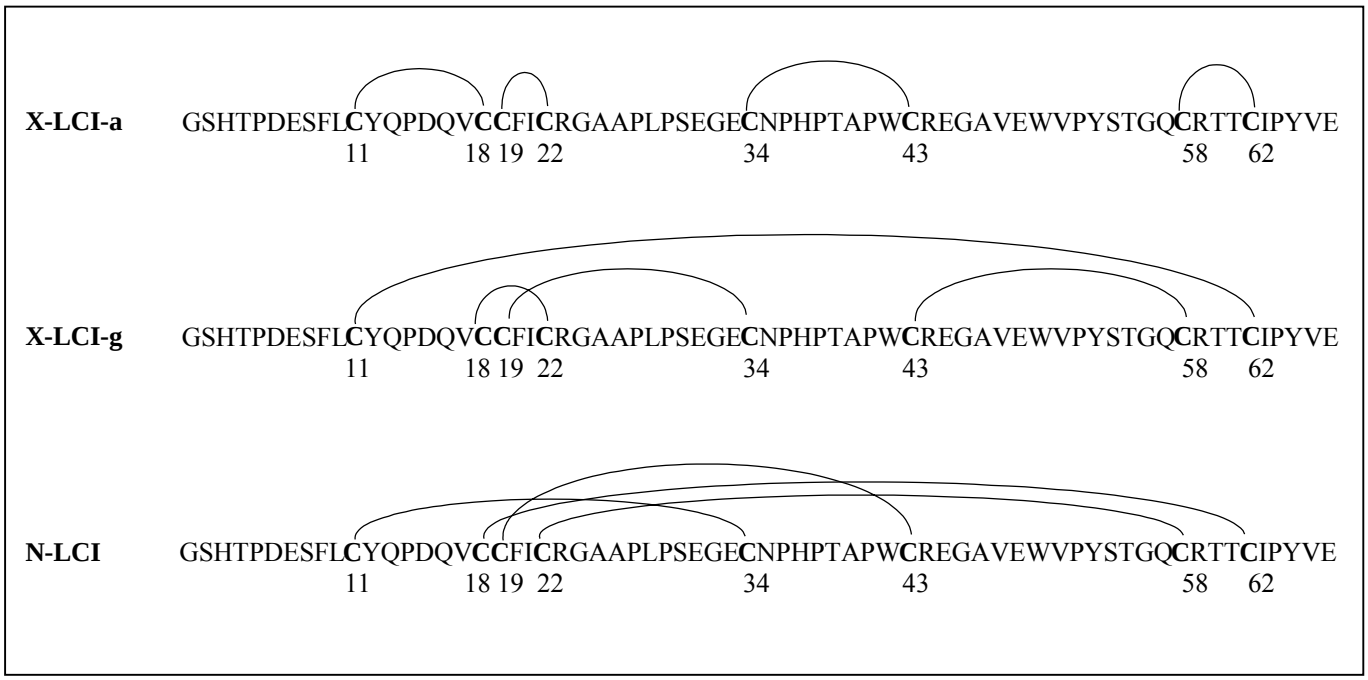

Figure 5. Disulfide structures of the native and scrambled LCI. The structures of X-LCI-a and X-LCI-g are d erived from Edman sequencing and mass analysis of disulfide-containing peptides of thermolysin-digested samples. Note that X-LCI-a corresponds to the beads-form. The disulfide pairing of the native LCI (N-LCI) is shown at the bottom for comparison.

IV.C.6. Kinetics of LCI Unfolding in the Presence of GdnHCl.

Given that GdnHCl concentration was found to be proportional to the amount of denatured PCI in terms of accumulated scrambled species, the kinetics of unfolding of the native LCI was studied at different denaturant strengths (Fig. 6). The unfolding of LCI is complete in 120 min at 8 and 7 M GdnHCl, whereas it takes 300 min to complete in 6 M GdnHCl. A significant difference can thus be achieved by slightly modifying the concentration of certain denaturant. The rate constant of unfolding at 8 and 7 M GdnHCl (3.3 × 103 min1) is about 2.5-fold greater than that observed at 6 M GdnHCl (8.3 × 103 min1).

Table I. Structures of disulfide-containing peptides derived from thermolysin digestion of scrambled LCI

Peptides a-n and g-n correspond, respectively, to thermolysin digestion products of X-LCI-a and X-LCI-g. The complete sequences of each peptide are shown, and the residues analyzed by Edman degradation are underlined. Sequence numbering refers to the recombinant LCI that contains a construction-added Gly as the N-terminal residue.

Peptide	Sequence	**Sequence position**	Cys-Cys	M_r found (exp.)
a-4	LCYQPDQVC	10-18	Cys^{11}-Cys^{18}	1066.22 (1067.22)
a-9	GECNPHPTAPWCREGAVEWVP	32-52	**Cys^{34}-Cys^{43}**	2333.59 (2333.09)
	TGQCRTTCIPYV	55-66	Cys^{58}-Cys^{62}	1339.56 (1339.61)
	ECNPHPTAPWC	33-43	Cys^{34}-Cys^{43}	1252.40 (1252.16)
a-10	AAPLPSEGECNPHPTAPWCREG	25-46	Cys^{34}-Cys^{43}	2317.55 (2316.51)
a-12	DESFLCYQPDQVCCFICRGA	6-25	Cys^{11}-Cys^{18}	2293.61 (2294.56)
			Cys^{19}-Cys^{22}	
a-13	DESFLCYQPDQVCCFICRGAAPLPSEGECNPHPTAPWCREGAVEWVPYSTGQ	6-57	Cys^{11}-Cys^{18}	5740.39 (5739.97)
			Cys^{19}-Cys^{22}	
			Cys^{34}-Cys^{43}	
g-5	CFI	19-21	Cys^{19}-Cys^{34}	1866.06 (1865.34)
	APLPSEGECNPHPTA	26-40		
g-8	CYQ	11-13	Cys^{11}-Cys^{62}	1328.58 (1328.72)
	RTTCIPYVE	59-66		
	WCREGAVEWVPYSTGQCRTT	42-61	Cys^{43}-Cys^{58}	2329.60 (2329.99)
	GAAPLPSEGECNP	24-36	Cys^{34}	1241.34 (1241.27)
g-9	PDQVCCFICRGAAPLPSEGECN	14-35	Cys^{18}-Cys^{22}	2309.65 (2309.94)
			Cys^{19}-Cys^{34}	
g-11	PWCREGAVEWVPYSTGQCRTT	41-61	Cys^{43}-Cys^{58}	2426.72 (2426.39)

IV.D. DISCUSSION

IV.D.1. LCI Conformational Stability.

The denaturation curves obtained by representing the fraction of native LCI converted into the scrambled species under increasing concentrations of denaturants (chaotropic agents, organic solvents, and temperature) are indicative of the conformational stability of LCI. GdnHCl and GdnSCN denature LCI quantitatively in a cooperative manner at concentrations between 2-3 and 3-4 M, respectively, in accordance with the observations made in the case of

cardiotoxin III (CTX-III) *(12)*, an all β-sheet protein. These values are higher than those obtained for PCI, another disulfide-containing carboxypeptidase inhibitor *(9)* that is almost devoid of any regular secondary structure, *(13, 14).* The higher concentration of denaturants required for LCI could reflect the contribution of secondary structure to the stability of the LCI fold. The higher stability of LCI compared with PCI is also shown by the fact that urea is unable to denature LCI, whereas PCI reaches 50% denaturation at 8 M urea *(9).* At this point it should be mentioned that the increase in fluorescence intensity observed in urea-treated LCI (Fig. 3) is not indicative of denaturation, because no significant red shift is observed between 0 and 8 M. However, a red shift (from 354 to 360 nm) is clearly observed in the 8 M GdnHCl-denatured LCI, which additionally shows a decreased fluorescence intensity. Thus, the increase in fluorescence intensity in urea-treated samples may be indicative of a different hydrophobic environment of tryptophan residues upon urea treatment generated by the dynamic relocation of secondary structure elements.

PCI, although less stable than LCI, is still a very stable fold with its globular structure stabilized by a compact hydrophobic core and by three disulfide bridges forming a T-knot. Both carboxypeptidase inhibitors are designed to resist extreme external conditions and still be functional. The comparison between the stabilities of other disulfide-containing proteins studied by this method is shown in Table II and is expressed as the concentration of denaturant required to achieve 50% of denaturation of the protein. The following two crucial aspects of these data obtained with seven different disulfide-containing proteins need to be mentioned. 1) The extent of denaturation achieved by each fold is dependent upon the type of denaturant. GdnHCl is generally more potent than urea, albeit the relative potencies vary from protein to protein. The two extreme examples correspond to LCI (in which urea is unable to quantitatively unfold LCI) and TAP, where urea is more potent than GdnHCl. The clear difference of potency between urea and GdnHCl has been extensively reported and can be attributed to the differential mode of action between these denaturants, although the detailed mechanisms are not yet fully understood *(11, 15, 16, 17).* It is known that both denaturants disrupt noncovalent interactions that stabilize the native fold *(18),* mainly hydrophobic interactions, by causing water to become a better solvent for nonpolar amino acids. In addition to this common property, GdnHCl is a salt and also suppresses electrostatic interactions. The suppression of electrostatic interactions is fundamental to achieve unfolding of an all β-sheet protein, as is the case for LCI. 2) LCI is globally the more stable protein studied by this method as yet. In addition to the inability of urea to denature it, no denaturation was observed either with 65% methanol or by heat treatment (incubation at 65

°C for 1 h). The high stability of LCI arises from an optimal combination of disulfide-bonding, a compact hydrophobic core, and the high percentage of regular secondary structure. This high conformational stability of LCI in extreme conditions would greatly facilitate its application to human therapy as a profibrinolytic agent.

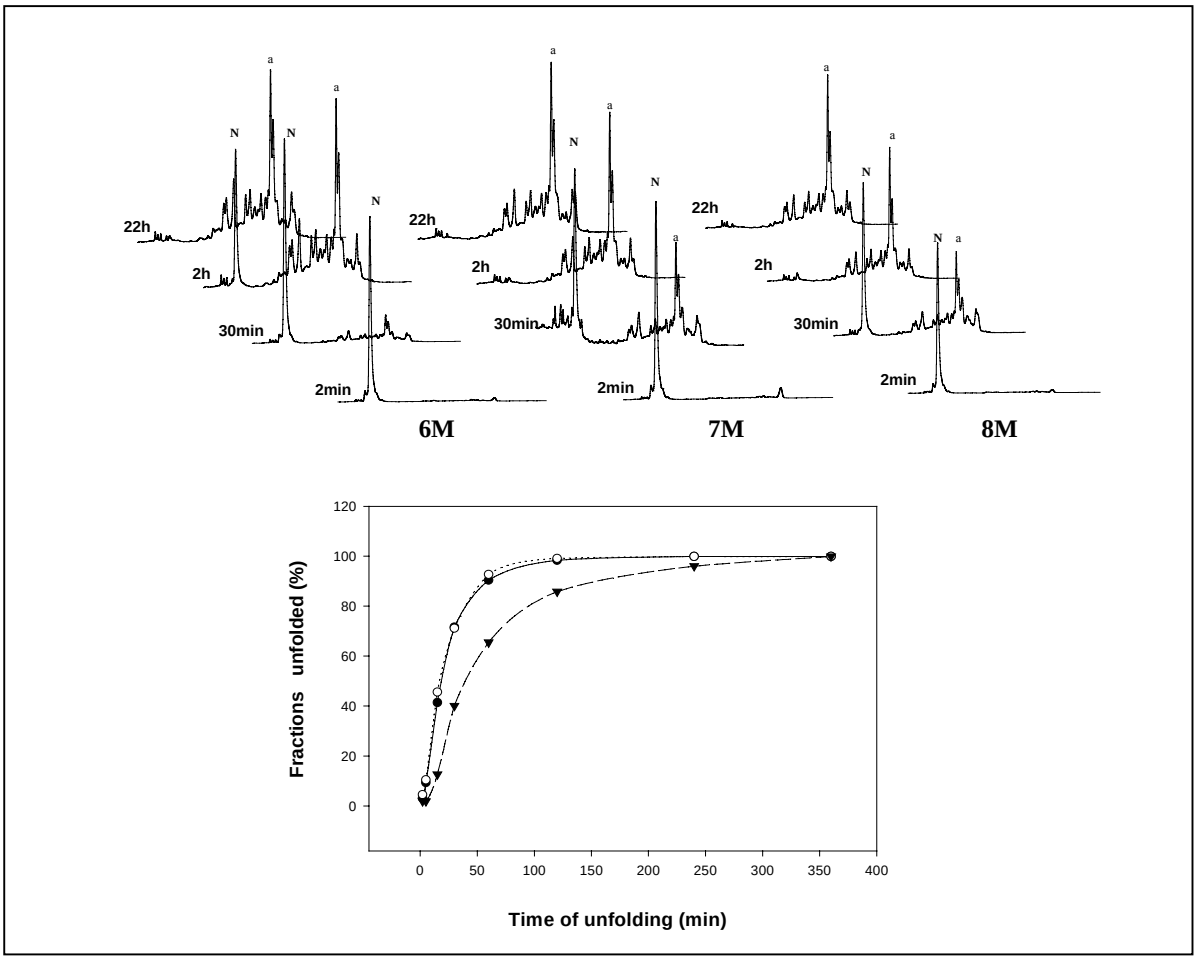

Figure 6. Time course unfolding of LCI. The reactions were performed in Tris-HCl (0.1 M, pH 8.4) containing 2-mercaptoethanol (0.25 mM) and different concentrations of GdnHCl. The denatured samples were quenched and analyzed as shown in Fig. 1. A) RP-HPLC kinetic analyses of samples denatured (unfolded) by different concentrations of GdnHCl. B) Kinetics of unfolding of LCI at 8 M (❍), 7 M (●), and 6 M (▼) of GdnHCl. The amount of unfolded protein is expressed as the total amount of scrambled species accumulated at the times stated.

IV.D.2. The Unfolding Pathway of LCI.

The denatured LCI was found to be composed of at least 9 scrambled isomers out of the possible 104 (Fig. 1). The unfolding pathway of LCI was determined by the evolution of the scrambled isomers generated under increasing concentrations of GdnHCl and GdnSCN (Fig. 4). Although the absolute amounts of each scrambled in the unfolding pathway is characteristic of the denaturant assayed, the composition and evolution of the different scrambled species is comparable. This indicates that these scrambled species correspond to

the main transient intermediates in the unfolding pathway of LCI. Since for an unfolding reaction the strong denaturation condition precludes the accumulation of any intermediate *(19),* the characterization of unfolding intermediates is only possible in disulfide-containing proteins. There are two populations of scrambled species that undergo variations along the unfolding pathway. One accumulates under strong denaturing conditions. This was the case for X-LCI-a and to a lesser extent for X-LCI-b. The other population shows an inverse correlation between their relative abundances and the denaturing conditions. This is the case for X-LCI-f, X-LCI-h, and X-LCI-g, the latter being the most populated scrambled at low concentrations of denaturant. Following previous results obtained with PCI *(9),* TAP *(8),* and insulin-growth factor (IGF-1) *(10),* an open or relaxed structure is expected to be found for the first population (including X-LCI-a and X-LCI-b) that could explain the prevalence of both forms in high concentration of denaturants. In contrast, the population represented by X-LCI-g should have another kind of non-native structure that turns unstable at high denaturant strength. These non-native structures are likely to be more compact than the unfolded state. The assignment of the disulfide structure of the most abundant scrambled species within each population has confirmed these hypotheses (Fig. 5). The identification of X-LCI-a as the beads-form isomer was already expected from similar results found with other proteins, such as PCI *(9),* TAP *(8),* and IGF-1 *(10),* which also show a predominance of the bead-form isomer under strong denaturing conditions. This can be due to a common pathway of unfolding where the polypetide chain undergoes a progressive expansion and relaxation toward the shape of linear structure. In contrast, X-LCI-g is an unstable intermediate with a quite compact non-native structure, since the N- and C- terminal ends of the molecule have already been brought together, as suggested by the pairing of disulfide bonds.

Table II. Concentration of different denaturants required to achieve 50% of denaturation of several disulfide-containing Proteins

These data were determined by the method of disulfide scrambling between the native and scrambled isomers. The data has a S.D. ± 5%. The references are described in the text.

Protein	GdmSCN (*M*)	GdmHCl (*M*)	Urea (*M*)
LCI	2.4	3.6	No denaturation
PCI	0.7	1.45	>8
RNase A	0.75	2.25	5.75
TAP	1.0	4.2	4.0
IGF-1	1.5	3.2	5.5
Hirudin	2	5	>8
CTX-III	Not determined	2.3	3.4

IV.D.3. Kinetics of LCI Unfolding.

The rate constant for unfolding of LCI at 7 and 8 M GdnHCl was found to be very similar, whereas it is about 2.5-fold lower at 6 M. Thus, a significant difference can be achieved by slightly modifying the concentration of certain denaturant. On the other hand, the variation of the rate constant of unfolding upon increasing concentrations of denaturants is not linear. This is in contrast not only with the behavior of proteins lacking disulfide-bonding *(19)* but also with the unfolding kinetics of CTX-III *(12)* in which there is a linear decrease of the rate constant for unfolding under denaturation by the same denaturant. The abrupt change in the rate constant for unfolding in LCI between 6 and 7 M GdnHCl could be an indication of the cooperative nature of the process and points out the relevance of hydrogen-bonding (regular secondary structure) in maintaining the native structure of LCI. On the other hand, the kinetics of LCI unfolding is about 15-25-fold slower than that of CTX-III *(12).* This could be one of the explanations for the high stability of LCI, although a refolding kinetics analysis is needed to confirm this hypothesis.

The results presented in this study confirm that LCI fulfills the basic requirements of high stability and slow kinetics of unfolding that are expected for a protein molecule with potential applications in human therapy.

IV.E. REFERENCES

1. Reverter, D., Vendrell, J., Canals, Q., Horstmann, J., Avilés, F. X., Fritz, H., and Sommerhoff, C. P. (1998) *J. Biol. Chem.* 273, 32927-32933.
2. Wang, W., Nagashima, M., Schneider, M., Morser, J., and Nesheim, M. (1998) *J. Biol. Chem.* 273, 27176-27181.
3. Bajzar, L. (2000) *Arterioscler. Thromb. Vasc. Biol.* 20, 2511-2518.
4. Reverter, D., Fernández-Catalán, C., Baumgartner, R., Pfänder, R., Huber, R., Bode, W., Vendrell, J., Holak, T. A., and Avilés, F. X. (2000) *Nat. Struct. Biol.* 7, 322-328.
5. Haber, E., and Anfinsen, C. B. (1962) *J. Biol. Chem.* 237, 1839-1844.
6. Anfinsen, C. B. (1973) *Science.* 181, 223-230.
7. Chang, J.-Y. (1997) *J. Biol. Chem.* 272, 69-75.
8. Chang, J.-Y. (1999) *J. Biol. Chem.* 274, 123-128.
9. Chang, J.-Y., Li, L., Canals, F., and Avilés, F. X. (2000) *J. Biol. Chem.* 275, 14205-14211.
10. Chang, J.-Y., Marki, W., and Lai, P. H. (1999) *Protein Sci.* 8, 1463-1468.

11. Pace, C. N. (1986) Methods Enzymol. 131, 266-280 Chang, J.-Y., Kumar, T. K. S., and Yu, C. (1998) *Biochemistry.* 37, 6745-675113.
12. Rees, D. C., and Lipscomb, W. N. (1982) *J. Mol. Biol.* 160, 475-498.
13. Clore, G. M., Groneborn, A. M., Nilges, M., and Ryan, C. A. (1987) *Biochemistry* 26, 8012-8023.
14. Tanford, C. (1968) *Adv. Protein Chem*. 23, 121-282.
15. Pace, C. N., Laurents, D. V., and Thomson, J. A. (1990) *Biochemistry.* 29, 2564-2572.
16. Liepinsh, E., and Otting, G. (1994) *J. Am. Chem*. Soc. 116, 9670-9674.
17. Dill, K. A., and Shortle, D. (1991) *Annu. Rev. Biochem*. 60, 795-825.
18. Matouschek, A., Serrano, L., and Fersht, A. R. (1992) *J. Mol. Biol*. 224, 819-835.

V. TRABAJO 3.

Identification of leech carboxypeptidase inhibitor (LCI) as a novel potent enhancer of t-PA mediated fibrinolysis through TAFI inhibition

V.A. INTRODUCTION

Dissolution of fibrin clots is the central strategy in the short-term clinical treatment of blood clotting disorders, particularly in acute myocardial infarction. Thrombolytic agents that are very effective in converting plasminogen into plasmin are used clinically to dissolve clots *(20).* Plasmin, the key protease in the fibrinolytic system, degrades the fibrin clot into soluble peptides that are cleared by the macrophage-monocyte system**.** Different agents have been studied and compared to improve thrombolytic therapeutic approaches. Currently, recombinant t-PA is the most widely used thrombolytic agent for the treatment of acute myocardial infarction (AMI). Unlike other compounds, t-PA is relatively clot specific and binds to fibrin-bound plasminogen, thus converting plasminogen to plasmin only at the surface of the fibrin, which is subsequently degraded. For this reason, t-PA is supposed to cause less bleeding side effects than non-specific agents such as streptokinase and urokinase. Unfortunately results of different trials indicate that although this therapy increases the survival of patients with AMI, its efficacy is limited, and only 50 % of patients achieve the complete and sustained reperfusion of the thrombosed artery *(1).*

The thrombus resistance has been attributed to the co-generation of thrombin *(1)* which, besides contributing to the production of new fibrin, may also catalyze the activation of plasma procarboxypeptidase B, also known as TAFI (thrombin activatable fibrinolysis inhibitor). Accumulating evidence in the last few years suggests that TAFI, a zymogen that circulates as such in plasma and is converted into its active form upon coagulation, constitutes a link between coagulation and fibrinolysis and mediates a potent anti-fibrinolytic activity *(2, 3).* Although activated TAFI (TAFIa) may also inactivate plasmin *(4),* its main physiological action seems to be is that of removing the newly exposed C-terminal Lys residues of fibrin, after been this molecule partially degraded by plasmin. Such Lys residues bind both plasminogen and t-PA with high affinity *(5)* and, therefore, the presence of active TAFI reduces the fibrin surface-specific production of plasmin and the resulting fibrin clot lysis.

The use of inhibitors that prevent the anti-fibrinolytic activity of TAFI has been shown to enhance the rate of clot dissolution induced by t-PA *(1).* Potato carboxypeptidase inhibitor (PCI), a 39 amino acid protein isolated from potato tuber that is a specific inhibitor of both the A and B types of the metallo-carboxypeptidase family of proteases, is one of the TAFI inhibitors that have been evaluated. A number of reports have provided convincing evidence for the effect of PCI in accelerating the t-PA-induced fibrin clot lysis *in vitro.*

Subsequent studies on several animal models have shown that co-administration of PCI and t-PA significantly enhances the efficacy of t-PA induced thrombolysis *(6-10).*

In an attempt to identify other agents as an alternative to PCI, we have evaluated the effects of a new proteinaceus carboxypeptidase inhibitor from leeches, LCI, on t-PA induced lysis of human plasma clots *in vitro*. LCI has been recently isolated and characterized by our groups *(11,12),* showing that is a 66-residue protein, with four disulfides with no sequence similarities to other known proteins, except at its C-terminal short tail (the main inhibitory site), which is similar to that of PCI. We have also described its efficient recombinant production and its detailed, three-dimensional structure (isolated and bound to a human carboxypeptidase) which is very different to that of PCI *(34).* Compared to PCI, LCI has a 10-fold higher affinity for the pancreatic carboxypeptidases A1, A2, and B and is very potent in TAFI inhibition *in vitro (11).* Therefore, it is expected that LCI could be particularly efficient as enhancer of t-PA thrombolytic therapy. The present study supports this assumption, showing that LCI significantly accelerates the rate of clot lysis induced by t-PA, through the affectation of TAFI activity.

Given that the susceptibility or resistance of fibrin to plasmin digestion is dependent on the organization of the fibrin network *(14, 15),* we have also studied the structural changes that occur in such network during fibrin polimerization and fibrinolysis in human plasma when TAFI is active or inactive. This has been done in the absence or the presence of either LCI or PCI and by scanning and transmission electron microscopy. A significant modification of fibrin clot architecture has been observed. When both inhibitors are enclosed, in agreement with the other clot lysis assays. On the overall, this study is the first description of the TAFI modulation by the novel carboxypeptidase inhibitor LCI. It supports the potential interest of this natural inhibitor as a drug or a lead compound for t-PA based thrombolytic therapies or related approaches.

V.B. EXPERIMENTAL PROCEDURES

V.B.1. Chemicals.

The synthetic carboxypeptidase substrate hyppuryl-L-Arg and the inhibitor D-Phe-Pro-Arg chloromethyl ketone (PPACK) were purchased from Bachem (Bubendorf, Switzerland). Human thrombin (10 NIH/ml) was from Sigma Co. (St.Louis, MO, USA). Rabbit lung thrombomodulin was obtained from American Diagnostica (Greenwich, CT). The recombinant human tissue-type plasminogen activator (rt-PA, alteplase, 145000 U/ml) used

was Actilyse from Boehringer Ingelheim (Ingelheim, Germany). All other chemicals not specifically noted were reagent grade.

V.B.2. Production of recombinant proteins.

Large scale recombinant production and purification of PCI and LCI from transformed *E.Coli* where carried out as previously described *(11,17).* The purity and homogeneity of the proteins was greater than 95%, as assessed by HPLC and mass spectrometry MALDI-TOF. Aliquots of protein samples were lyophilized and stored at -20ºC. Both proteins were prepared as concentrated stock solutions (1mg/ml) and diluted in phosphate buffer saline (PBS) just before use.

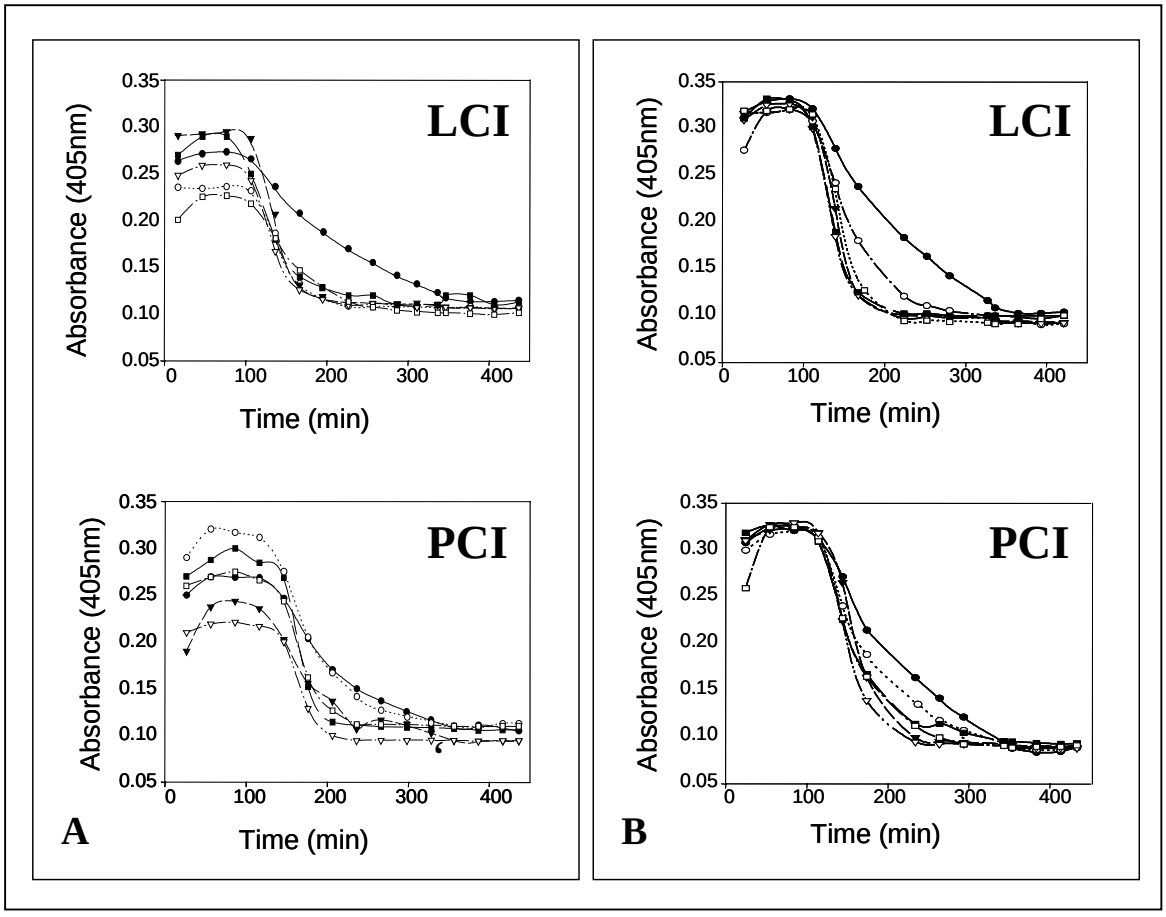

Figure 1. Profibrinolyitic effect of LCI compared to PCI in plasma clot lysis assay. Human plasma was clotted using an equimolar mixture of thrombin plus trombomodulin: 1.1 U/ml (figures A1 and B1); 2.2 U/ml (figures A2 and B2). Fibrinolysis curves were determined following the turbidity as described in Material and Methods. Plasma was previously incubated with serial concentrations of LCI in figure A: (●) control 0nM , (O)30nM, (▼)50nM, (▽) 70nM, (■)90nM, (□)110nM; or PCI in figure B plasma was previously incubated with serial concentrations of PCI: (●) control 0nM , (O) 30nM, (▼)250nM, (▽) 500nM, (■)700nM, (□)1μM. Each point represents the mean of 5 independent experiments.

V.B.3. Plasma samples.

Pooled normal plasma was obtained by mixing plasma from 50 healthy volunteers. Blood samples were obtained by venipuncture from the antecubital vein and was immediately anticoagulated with 1/10 volume of 0.129M sodium citrate. To obtain platelet-poor plasma the blood samples were centrifuged twice at 2500g for 15 min. Plasma samples were stored at –80ºC until use.

V.B.4. Inactivated serum.

Normal sera from 50 healthy volunteers were pooled together and placed for 30 minutes at 56ºC, resulting in the complete loss of all basic carboxypeptidase activity.

V.B.5. Plasma clot lysis assay.

Clot lysis was studied in a plasma system in which t-PA-mediated fibrinolysis of a thrombin-induced clot is measured by a turbidimetric method *(16)*. Briefly, citrated plasma was diluted with PBS (1:4). Various concentrations of test agents (LCI or PCI) in a range between 30nM and 1μM were added to diluted plasma. After thorough mixing, 100μl of this mixture was immediately transferred to the well of a microtiter plate containing 100 μl of a solution containing $CaCl_2$, t-PA, thrombin, and thrombomodulin and incubated at 37°C. Final concentrations were $CaCl_2$ 5.7 mM, t-PA 0.054 U/ml, thrombin 1.12 IU/ml or 2.2 IU/ml, and thrombomodulin 1.12 U/ml or 2.2 U/ml. Conditions of each fibrinolysis curve are described in the legend of Fig. 1. In another series of assays, no thrombomodulin was added and the concentration of thrombin was maintained at 1.12 IU/ml or 2.2 IU/ml. The absorbance at 405nm was measured at 37ºC using an A-5022 Anthos microplate reader (Anthos labtec intruments, Salzburg) at 30 minutes intervals for 6 hours. Clot lysis time was defined as the time elapsed between the maximum turbidity and the midpoint of the maximum turbid-to-clear transition that characterizes the lysis of fibrin.

V.B.6. Determination of TAFI activity.

TAFI (plasma carboxypeptidase B) activity in plasma was determined using a method based on the colorimetric determination of hippurate released by the enzyme with cyanuric chloride/dioxan reagent *(16)*. In every experiment a standard curve of the TAFI activity in normal plasma was determined by serial dilutions of normal plasma in heat inactivated serum, whereas plasma samples were determined in duplicate using two dilutions of plasma in heat inactivated serum (75% and 50% plasma).

Since TAFI activation depends on the amount of thrombin and thrombomodulin added to plasma *(2),* the carboxypeptidase activity determination in normal plasma was carried out reproducing thrombin and thrombomodulin concentrations used to activate TAFI in the clot lysis assay (1.12 IU/ml or 2.2 IU/ml, final concentrations). To initiate TAFI activation thrombin, thrombomodulin and $CaCl_2$ (17mM) were added to 30µl of normal plasma containing no inhibitors or either LCI (110nM) or PCI (500nM), and the volume was adjusted to 60µl with 20mM HEPES (N- [2-hydroxymethyl]-piperazine-N'-[2-ethanesulfonic acid], pH 7.4) buffer containing 150mM NaCl, 5mM $CaCl_2$. After 10 min incubation at room temperature, the activation of TAFI was stopped by addition of PPACK (D-Phe-Pro-Arg chloromethyl ketone) (20µl, 150µM). Hippuryl-Arg, the substrate for carboxypeptidase B activity, was added, (20µl, 20µM) and after thorough mixing conversion to hippuric and was allowed for 10 minutes. The substrate reaction was stopped by adding 20µl of 1M HCl followed by addition of an equal volume of 1M NaOH. 25µl of 1M sodium phosphate (pH 7.4) was added to each sample to fulfil the phosphate requirements of the colorimetric determination of hippurate with cyanuric chloride/dioxan. Finally, 60µl of 3% cyanuric chloride dissolved in 1,4-dioxan was added and colour was allowed to develop under extensive vortexing. The incubation mixture was centrifuged at 14000rpm for 2min to remove denatured protein and excess cyanuric and 100µl of each sample was transferred to a microtiter plate. Absorbance was measured at 405nm in an A-5022 Anthos microplate reader (Anthos labtec intruments, Salzburg)

To distinguish between the constitutive carboxypeptidase activity (CPN) and the inducible carboxypeptidase activity (TAFIa) in plasma, the TAFIa activity was calculated as the carboxypeptidase activity sensitive to inhibition by a saturating concentration of PCI (25µg/ml). The remaining enzymatic activity at PCI saturating concentration was taken as CPN constitutive activity and substracted from total carboxypeptidase activity obtained at every sample. TAFI activities in plasma samples were expressed as a percentage of the TAFIa concentration in normal plasma.

V.B.7. Scanning electron microscopy (SEM).

Clots were examined during the rapid phase of fibrin assembly and fibrinolysis when profound differences between turbidity of control clots and clots treated with LCI or PCI were observed. 2.2 U/ml of thrombin and thrombomodulin were used to initiate coagulation and activate TAFI. Six time points of the fibrinolysis curve were selected for SEM analysis.

Microdroplets of plasma clots were placed in a well dish covered with parafilm, thoroughly washed with PBS and immediately treated with the primary fixative (2% glutaraldehyde in 0.1M PBS, pH 7.4) at selected times. After post-fixation in 1% osmium tetroxide in PBS for 90 minutes, they were dehydrated in acetone and critical-point dried. Samples were rotary shadowed with gold and subsequent microphotographs of representative areas were taken on a Hitachi s-570 (Hitachi LTD. Tokyo, Japan) scanning electron microscope. Micrographs magnification are shown at Fig. 4 legend. Fibrin fibers thicknesses were analyzed from micrographs using Metamorph, Version 4.6r5. Universal Imaging Corporation, Lisensed under U.S.Patent N.4, 558,302.

IV.B.8. Transmission electron microscopy (TEM).

Microdoplets of plasma clots (prepared and selected as described above) were applied to carbon grids and negatively stained with 2% uranyl acetate. Images were taken in a JEOL 1200EX-II electron microscope operated at 100KV and recorded on Kodak SO-163 film at 60,000 nominal magnification.

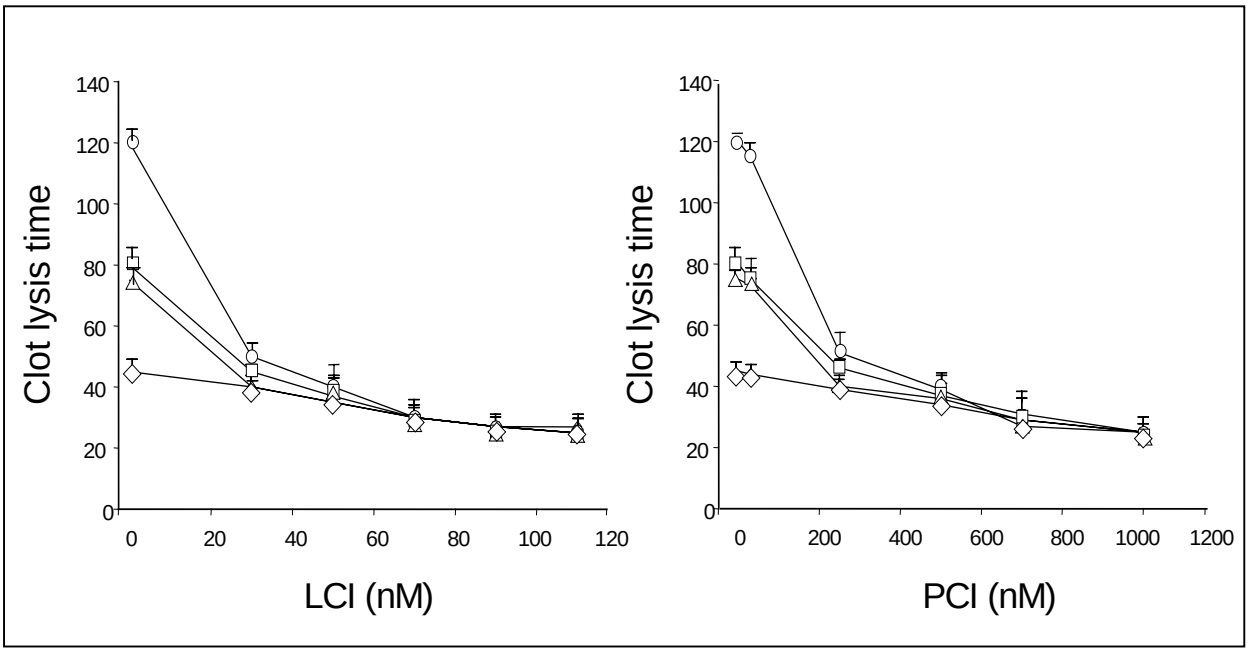

Figure 2. Effect of PCI and LCI on clot lysis time. Human plasma was clotted in presence of different concentrations of thrombin or thrombin plus thrombomodulin: (◇) 1,12 U/ml thrombin, (Δ) 2,2 U/ml thrombin, (□) 1,12 U/ml thrombin and trombomodulin, (O) 2,2 U/ml thrombin and thrombomodulin. Each point represents the mean ± SEM of 5 independent experiments. Left panel: effect of LCI at concentrations ranging from 30 to 110nM. Right panel: effect of PCI at concentrations ranging from 30nM to 1μM.

V.C. RESULTS

V.C.1. The importance of properly produced protein inhibitors.

Both PCI and LCI are small disulfide-rich proteins, which can generate multiple disulfide-paired forms, most of them scrambled and poorly active towards their target enzymes (metallo-carboxypeptidases), if they are not properly folded and stored *(11, 17, 33, 35)*. When obtained from natural sources, they can have further heterogeneity, as it is the case of PCI, which occurs in potato as several isoforms *(31)*. To overcome such problems we have produced both PCI and LCI from cDNAs cloned and characterized in our groups *(11, 30),* by recombinant systems previously reported *(11,16)* followed by refolding procedures in presence of different redox conditions *(35)*. HPLC and MALDI-TOF analysis *(32)* assured a purity and conformational homogeneity of the protein inhibitor samples greater than 95-98%, confirmed by enzymatic inhibitory activity analysis. Storage in frozen solution at -80ºC assured maintenance of these properties.

V.C.2. *In vitro* effect of LCI on plasma clots.

Clot formation was induced in human plasma from healthy individuals by adding thrombin or thrombin/thrombomodulin to the system, and the process was followed by measuring the absorbance values periodically. The turbidity of the samples initially increases with clot formation to progressively decrease as t-PA-induced fibrinolysis takes over. Clot lysis time was determined by mathematical analysis of the derived lysis curve. To investigate the effect of LCI on t-PA-induced fibrinolysis, plasma clot lysis assays were conducted with increasing concentrations of the protein inhibitor, and the results were compared with a parallel set of assays in which PCI was used instead of LCI. The detailed dose-response studies are shown in Fig. 1A, for the set of experiments at 2.2 IU/ml of thrombin/thrombomodulin, which was the one in which cleaner effects were observed among the different assayed (see also Fig. 2 and methods). As expected, the clot lysis time significantly decreased along the dose range used for PCI (30 nM to 1 μM), in agreement with previous related studies with purified commercial PCI (6). A similar, but much stronger effect was observed with LCI since doses about ten times lower (ranging from 30 nM to 110 nM) are sufficient to achieve an equivalent fibrinolysis profile. The heterogeneity of the samples in the clotting region (0 to 100-150 min) makes difficult the comparison of absolute turbidity values among different curves, although each one has an internal coherence. Normalization of

the curves facilitates such comparisons (Fig. 1B), but may generate other inconsistencies, which must also be taken into account.

Accurate measurements of clot lysis time can be derived from mathematical analysis of the lysis curves obtained. Fig. 2 shows the estimated clot lysis time values for plasma treated with thrombin or thrombin/thrombomodulin at different concentrations in the presence of LCI or PCI. It may be observed that at the conditions at which clot lysis time is shorter (2.2 IU/ml of thrombin/thrombomodulin), which coincides with higher TAFI activation (see Fig. 2) LCI addition accelerates the process by a time factor of 4.8 (from 120 to 25 minutes) when a concentration of 90nM or higher is used. This decrease in clot lysis time is similar to the one observed with the addition of 800nM PCI. The ratio of approximately 1:10 LCI: PCI required to achieve a maximal acceleration in the fibrinolysis rate is maintained through the serial concentrations, even when not all of the TAFI present in plasma is active, thus confirming that, compared to PCI, LCI is a 10 fold more powerful fibrinolytic agent, in these conditions.

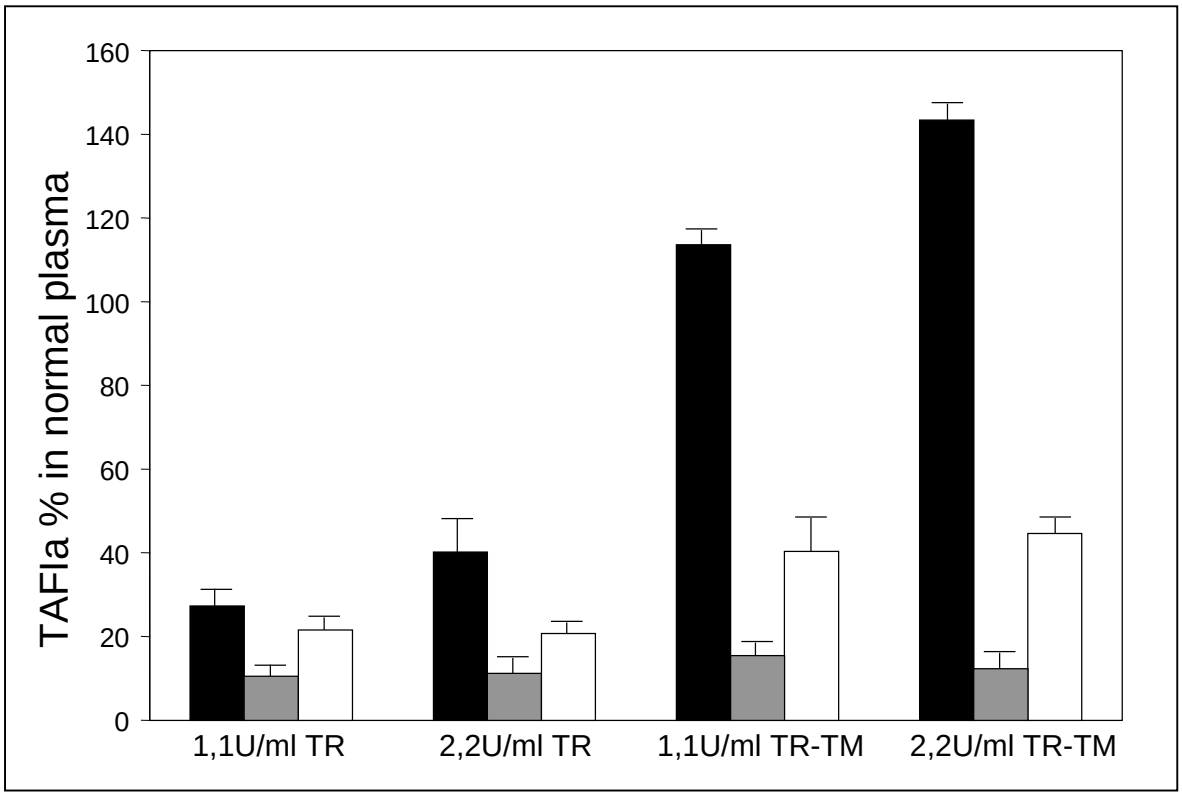

Figure 3. TAFI activity in control and LCI or PCI treated plasma. TAFI activity was determined in control human plasma (left bar, in black), plasma treated with 110nM LCI (middle bar, shadowed) and plasma treated with 500nM PCI (right bar, in white). After activation of TAFI with the different concentrations of thrombin or thrombin plus thrombomodulin shown below the histograms, TAFI activity was determined using hippuryl-Arg as substrate. Each point represents the mean $\pm$ SEM of 3 independent experiments

Regarding the different conditions to generate activated TAFI (TAFIa), it is interesting to note that clot lysis time appears to be much shorter in the presence of thrombin alone acting as both clotting trigger and TAFI activator (see the two bottom traces in both panels in Fig. 2). Also, in these cases there is no significant difference in the clot lysis time between the control and the LCI or PCI-treated samples. Apparently the thrombin/thrombomodulin complex is highly effective to achieve an optimal activation of TAFI, thereby releasing its antifibrinolytic activity. However thrombin alone is less effective and tends to destabilize TAFI, probably degrading it and annulating its antifibrinolytic effect. It is conceivable that, in the latter conditions, LCI and PCI are left without their target protease and their overall effect on fibrinolysis enhancement is much diminished.

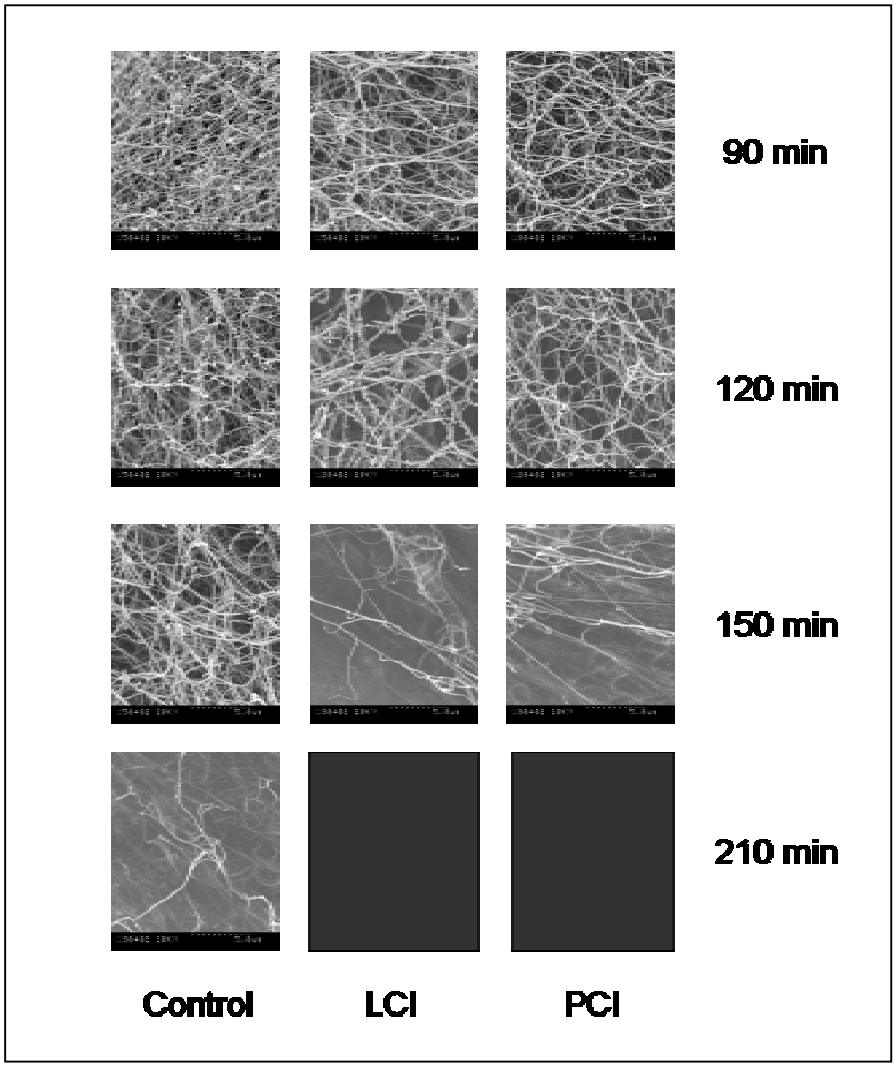

Figure 4. Scanning electron microscopy of plasma clots in LCI and PCI-treated plasma. Clots were prepared as described in the Materials and Methods section. The process of fibrin network formation and fibrinolysis was stopped by fixation with glutaraldehide at serial times in order to determine the structural differences in fibrin network between control clots and 110nM LCI or 1μM PCI treated clots. Each figure has a magnification corresponding to the scale indicated by the bottom bar that represents a distance of 5μm at micrographs.

V.C.3. LCI levels influence TAFI activity in plasma.

Recombinant LCI was tested for its ability to modulate TAFIa activity in human plasma. TAFI was activated by incubation in the presence of thrombin or the thrombin/thrombomodulin complex at the same conditions described in the plasma clot lysis assay, and the released activity was measured using the TAFI synthetic substrate hippuryl-Arg (specific for basic carboxypeptidases). To find out whether the inhibitor mediated fibrinolysis acceleration correlates with a similar direct quantitative effect on TAFI activity, LCI and PCI were added to the plasma and the activity of activated TAFI was measured. LCI was tested at a final concentration of 110nM, which is above the threshold of maximum effect on clot lysis time, while PCI was added at a concentration of 500nM. Fig. 3 shows that in these conditions, LCI leads to a strong inhibition of TAFI activity, independently of the conditions used to activate. In all the activation conditions tested, TAFI activity in the presence of LCI is half the value of that measured in the presence of PCI. This, together with the 5-fold difference in the dose of inhibitor used, accounts for an approximately 10-fold potency in the inhibitory activity of LCI as compared to PCI. The results correlate with those obtained in clot lysis time assays, confirming that the pathway of action of these inhibitors in plasma may be mediated by their specific binding to TAFI.

V.C.4. Effect of LCI on clot structure.

In parallel to the turbidimetric assays, scanning electron microscopy was used to visually compare the structures of control clots, containing fully active TAFI, and clots derived from LCI and PCI-treated plasma samples, in the search for morphological differences that may be correlated with the results described above. At given times, the process of assembly and destruction of the fibrin network was interrupted, samples taken and analysed by scanning electron microscopy (SEM). The corresponding micrographs are shown in Fig. 4. Overall, the fibrin network architecture appeared to be clearly different in control and treated samples, and the fibers formed in control clots were found to be consistently and significantly thinner (around 25%) than those formed in LCI-containing clots, as determined by using the program Metamorph (data not shown). As compared to control clots, inhibitor-treated samples showed as a less tight and dense network, with a weaker entanglement, and containing less clumps at all time-points assayed. By minute 90, when a maximum of fibrin polymerization is accomplished according to the turbidimetric data, network pores are barely visible and the fibers show a high degree of interlinking in control clots, whereas those treated with either LCI or PCI appear more ordered and less tightly packed. By minute 120, clearly in

the fibrinolysis side of the process, the protein inhibitors-treated samples show an increase in the number of large pores in the network as compared to the almost completely poreless control samples. Differences in network architecture are dramatic by minute 150, when clots arising from protein inhibitors-treated samples have been already completely disaggregated, while they are still clearly visible in control samples. Thus, LCI and PCI have a clear effect on the molecular structure of the fibrin clot, although requiring much lower doses in the first case. This enhancement of the fibrinolysis rate and efficiency is likely to be related to a facilitation of the liquid flow through the fibers resulting from the early appearance of large pores that leads to a more effective transport of fibrinolysis promoting components.

V.C.5. LCI does not appear to alter fibrin monomers assembly.

Transmission electron microscopy was finally used to analyze whether LCI treatment of human plasma could induce a noticeable alteration of the normal polymerization of fibrin monomers. Representative results are depicted in Fig. 5. By minute 5, at the early stages of fibrin network assembly, the most remarkable difference is the large amount of possible soluble protein that can be seen predominantly around the fibrin fibers in the LCI-treated clots, while fibers appear cleaner and better defined when active TAFI is present during the clot formation. At minute 50, LCI-treated samples appear to be dramatically different from the control clots. Treatment of human plasma with LCI results in clots made up of thicker fibers than control clots, where highly branched fibers and small, interlinked fibrils are visible. Larger pores are also noticeable in LCI-treated clots, which could contribute to an easy permeability of the fibrinolytic agents through the fibrin clot network. This suggests that incipient clots are formed and are soon dissolved in the LCI-treated samples. By minute 200, a number of long fibrin fibers are still present in untreated samples while virtually all of the fibrin fibers have disappeared from LCI-treated clots.

V.D. DISCUSSION

The knowledge of the structure and mechanisms for blood clots formation and disagregation still have a great interest nowadays, at both basic and applied levels. Regarding the evaluation of the nowadays risks of thrombosis therapies, important efforts are being devoted to treatments that target specific mechanisms of clot formation and dissolution. Despite the overall positive results of a number of thrombolytic agents that are currently being evaluated in randomized trials for the treatment of thrombosis disorders, some common

problems appear, such as thrombus resistance or bleeding side effects complications, regardless of the particular agent being used until now *(20,21).* In different animal models, the therapeutic value of t-PA treatment of thrombosis has improved by the simultaneous administration of a selective TAFI inhibitor *(7).* Given that the modulation of TAFI activity by specific inhibitors accelerates the lysis of fibrin clots induced by t-PA *(3, 9, 10),* a lower concentration of this thrombolytic agent might be needed to achieve a therapeutic effect with a subsequent reduction in the risk of bleeding *(21).* On the other hand, the control of TAFI activity is also of interest for preventive therapies because increased TAFI levels have been associated with an increased risk of thrombosis *(22, 23, 24).*

These considerations established a rationale for the characterization and development of novel TAFI inhibitors as adjuvants of currently available thrombolytic agents and for the prevention of thrombosis. LCI, a protein molecule first described and characterized by one of our group *(11-13)*, was tested with such a purpose and PCI was used as control because of its previously known efficiency as enhancer of t-PA fibrinolytic activity *(3).* Here we provide experimental evidence that the treatment of human plasma with recombinant LCI causes a complete inhibition of TAFI activity and significantly enhances the thrombolytic activity of t-PA *in vitro*. LCI is about 10 times more efficient than PCI as judged from the doses needed to attain the same TAFI inhibition levels.

A number of reports state that concentrations of PCI higher than the ones described in this work are needed to achieve the TAFI inhibition levels required as a thrombolytic *(24).* This might arise from the fact that in those studies commercial PCI was used (6), which might be heterogeneous in sequence and conformation. Our previous knowledge of the recombinant production, folding and structure-function relationships of both PCI and LCI *(11, 13, 17, 33, 36)*, showed us how to produce and use these proteins in a pure and biologically active state, thus allowing us to carefully titrate the amount of inhibitor used in the assays and to accurately establish the concentration ratio of both inhibitors. On the other hand, when TAFI activity has been measured in the same conditions used in clot lysis assays, it has been observed that the doses of added inhibitors required to achieve a maximum acceleration of the fibrinolysis rate are also optimal in the inhibition of the carboxypeptidase activity. This, together with the consideration of the need to use the complex thrombin/thrombomodulin both to attain a complete TAFI activation, and to avoid its premature degradation, confirm that TAFI plays a major role in fibrinolysis control and indicates that the use of new inhibitors like LCI could be of therapeutical value.

Several studies have previously provided convincing evidence for a role of PCI in thrombolytic therapies *in vivo*. For instance, PCI has been shown to enhance t-PA-induced clot lysis of thrombosis formed in arterio-venous shunt and in abdominal aorta in rat *(26)*. The efficiency of PCI in improving the t-PA induced arterial thrombolysis in rabbits and in the potentiation of endogenous thrombolysis in a jugular vein thrombosis model in rabbits has also been reported *(1, 6)*. The specificity of PCI allows it to act without affecting blood pressure, fibrinogen concentrations and blood coagulation. Whether the stronger power of LCI versus PCI as inhibitor of TAFI activity in human plasma clot lysis assay should be taken into account in therapeutic approaches, and whether its superiority is maintained *in vivo*, should be examined.

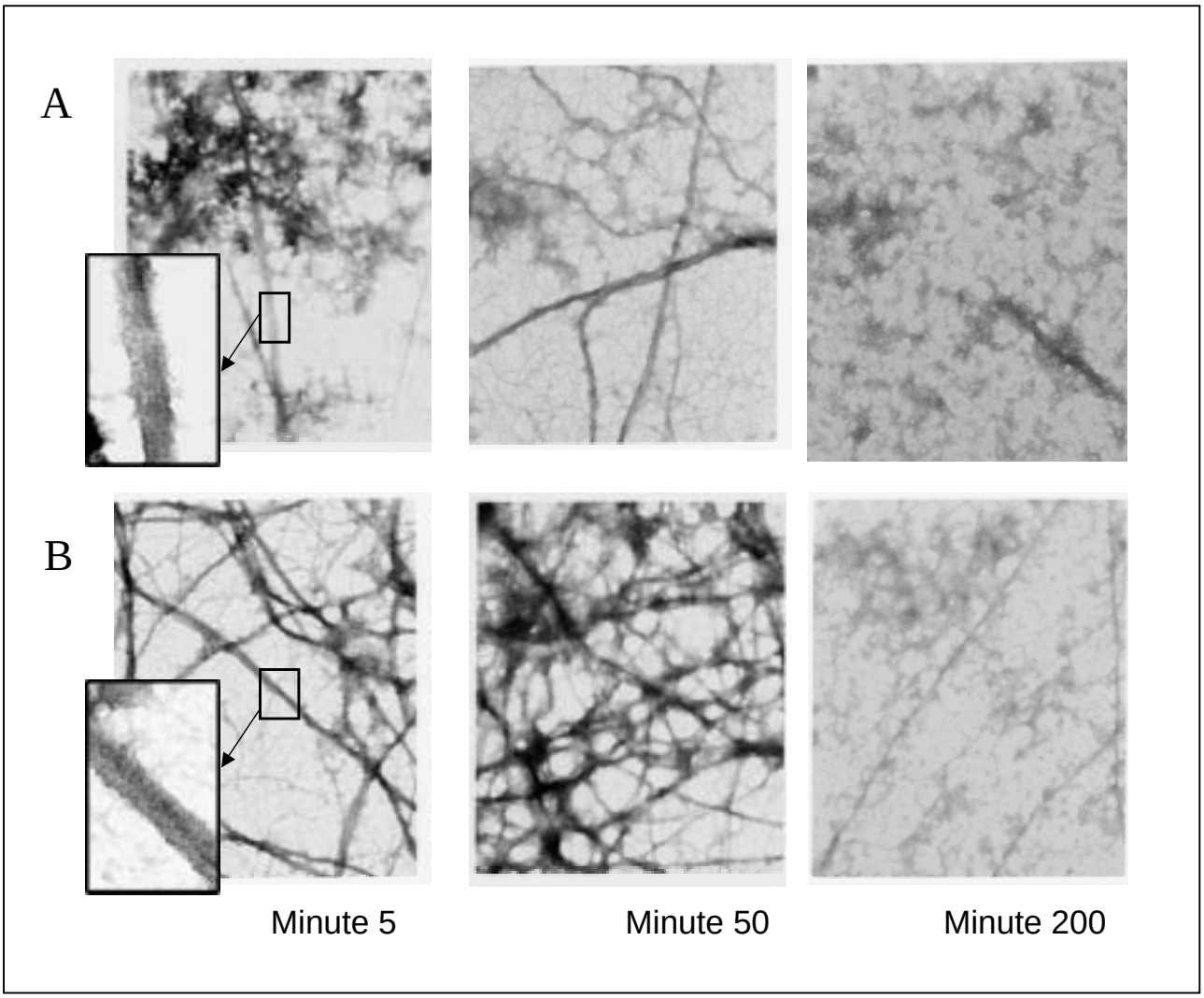

Figure 5. Transmission electron microscopy of plasma clots in control and LCI-treated plasma. Clots were prepared as described in the Materials and Methods section. Samples were analyzed at serial times to distinguish substructural differences in fibrin structure not seen by scanning electron microscopy. Figure shows the fibrin network in control clots (A) and 110nM LCI treated clots (B). Each figure has a magnification of 60,000.

The susceptibility of fibrin clots to plasmin degradation is dependent on how the clot network is formed and organized. Briefly, fibrin clots are formed after thrombin-mediated release of fibrinopeptides A and B from fibrinogen by plasmin, which results in the generation of fibrin monomers. Assembly of these monomers through non-covalent interactions leads to the formation of protofibrils *(27)*. Subsequent cross-linking reactions between the amide nitrogen of glutamines and ε-amino groups of lysines (Lys) of neighbouring fibrin molecules increases the mechanical strength and resistance of the clot *(18)*. Thus, it appears that a change in the conditions that lead to the initial non-covalent assembly of monomers could ultimately affect clot structure. On the other hand, cleavage of C-terminal Lys and Arg residues from fibrinogen is an accepted physiological action of TAFI that could interfere with the lateral aggregation of protofibrils. It is also well known *(29)* that defective polymerization may also be reflected in inadequate fibrinolysis. Properties like fiber thickness, pore size and fiber branching influence the diffusion rates of macromolecules such as plasminogen or t-PA within the fibrin network.

Previous studies by confocal microscopy using FITC-plasminogen *(3)* have shown that when plasma is clotted in presence of maximally activated TAFI, the lysis is approximately 5 times slower that in the absence of active TAFI, and it is not accompanied by a progressive accumulation of plasminogen on the surface of the fibrin fibers. Our experimental design to monitor the ongoing lysis of clotted plasma by scanning electron microscopy in the presence or the absence of specific TAFI inhibitors, allowed us to simulate a situation of TAFI inactivation, instead of generating inactive TAFI due to the absence of thrombomodulin in the experiment.

The scanning electron microscopy results presented here show that treatment of plasma with LCI or PCI results in clots made up of thicker fibers and larger pores. This altered clot architecture, observed in all time-points analyzed, might influence the rate of lysis. However, it is still unknown how do the changes in TAFI activity manage to alter the structure of the clot. It is known that less plasmin is found in clots composed of thin fibers as compared to thicker-fiber clots *(30)*. The decrease in plasmin levels also leads to a decreased rate of conversion of plasminogen into plasmin by t-PA, and to a subsequent lower rate of fibrinolysis *(2)*. Conversely, production of thick fibers is associated with adsorption of t-PA and increased fibrinolytic rates. These effects may be derived from either a decrease in plasmin-binding sites within thin fibers or to the fact that the access of plasmin to those residues is limited. TAFI could possibly affect fiber thickness through the elimination of plasminogen binding sites from partially degraded fibrin. It would generate thinner fibrils

devoid of Lys and Arg and unable to correctly proceed to the activation of plasminogen by t-PA, as happens in the control, active TAFI-containing experiments.

Analysis of the fibrin structure by transmission electron microscopy confirmed the results obtained by scanning electron microscopy, and the assumption about the changes in fibrin architecture due to the presence of LCI or PCI. However, this has been a preliminary study with such approach and with the limited resolution attained, the micrographs did not show noticeable differences in protofibril substructure, such as changes in lateral aggregation. Work is in progress to improve it. However, the differences observed in the fibrin branching already suggests that TAFI activity might indeed have some effect, not yet identified, in monomer assembly.

The data presented in this work clearly shows the capability of LCI to strongly inhibit TAFI in human plasma and, through this action, to speed up significantly the mechanism of fibrinolysis and the desagregation of fibrin clot structure. Also support the efficiency and specificity of LCI as a potent additive in currently available t-PA thrombolytic therapy. Our results further support recent reports that suggest the application of specific TAFI inhibitors in thrombolytic therapy *(1, 6).* Further *in vivo* studies with this class of inhibitors are justified and may provide the basis for their future clinical development.

In the present context, it is interesting to speculate whether LCI might be a potentially appropiate molecule for internal therapeutic use in humans, given that it comes from leeches, a blood-sucking parasite for mammals. To what extend the necessity of leeches to generate minimal local perturbations in the host when bite, it has led to an inmunological and toxicological adaptation of its molecules that are in contact with the bleeding point, is something that must be taken into account and that would merit further research.

V.E. REFERENCES

1. Klement P., Liao P., Bajzar L. (1999) *Blood.* 94, 2735-43.
2. Bajzar L., Morser J., Nesheim M.E. (1996) *J.Biol.Chem.* 271, 16603-8.
3. Sakharov D.V., Plow E. F., Rijken D.C. (1997) *J.Biol.Chem.* 272, 14477-14482.
4. Wang W., Hendricks D.F., Sharpe SS. (1994) *J.Biol.Chem.* 269, 15937-44.
5. Eaton D.L., Malloy B.E., Tsai S., Henzel W., Drayna D. (1991) *J.Biol.Chem.* 266, 21833-38.
6. Nagashima M., Werner M., Wang M., Zhao L., Light D.R., Pagila R., Morser J., Verhallen P. (2000) *Thrombosis Research.* 98, 333-42.
7. Klement P., Liao P., Bajzar L. (1998) *Blood.* 92, (Suppl 1): 709a.

8. Refino C.J., Schmitt D., Pater C., Eaton D., Bunting S. (1998) *Fibrinolysis and Proteolysis.* 12 (Supple 1): 29.
9. Minemma M., Friederich P., Levi M., von der Borne P., Mosnier L., Meijers J., et al. (1998) *J.Clin.Invest.* 101, 10-14.
10. Redlitz A., Nicolini F.A.,Malycky J.L., Topol E.J., Plow E.F. (1996) *Circulation.* 93, 1328-30.
11. Reverter D., Vendrell J., Canals F., Horstmann J., Aviles F.X., Fritz H., Sommerhoff C.P. (1998) *J. Biol. Chem.* 273, 32927-33.
12. Reverter D., Fernandez-Catalan J., Baumgartner R., Pfander X., Huber R., Bode W., Vendrell J., Holak T., Aviles F.X. (2000) *Nature Struct Biology.* 7, 322-28.
13. Salamanca S, Villegas V, Vendrell J, Li L, Aviles FX, Chang JY. (2002) *J.Biol.Chem.* 277, 17538-43.
14. Sakata Y., Aoki N. (1982) *J.Clin.Invest.* 69, 536.
15. Francis C.W., Morder V.J. (1988) *Blood.* 71, 1362.
16. Mosnier LO, Von dem Borne PAK, Meijers JCM, Bouma BN. (1998) *Thromb Haemost.* 80, 829-35.
17. Molina, M.A., Avilés, F.X., and Querol, E. (1992) *Gene.* 116, 129-138.
18. Gabriel D.A., Muga K., Boothroyd E.M. (1992) *J.Biol.Chem.* 267, 24259-63.
19. Antman E.M., for the TIMI 9A investigators. (1994) *Circulation.* 90, 1624-30.
20. Neuhaus K.L., Essen R.V., Tebbe U., Jessel A., Heindrichs H., Mourer W., Doring W., Hormjanz D., Kotter V., Kalhammer E., Simon H., Horace K.T. (1994) *Circulation.* 90, 1638.
21. Refino C.J., DeGuzman NL., Bunting S. (2000) *Fibrinolysis and Proteolysis.* 14, 305-13.
22. van Tilburg N.H., Rosendaal F.R., Bertina T.M. (2000) *Blood.* 95, 2855-59.
23. Schatterman KA., Goossens F.J., Sharpé S.S., Hendricks D.F. (1999) *Thromb.Haemostasis.* 82, 1718-21.
24. Boffa M.B., Reid TS., Joo E., Nesheim M.E., Koschinsky L. (1999) *Biochemistry.* 38, 6547-558.
25. Mosnier L., Meijers C.M., Bouma N. (2001) *Thromb Haemost.* 85, 5-11.
26. Hashimoto M., Yamashita T., Oiwa K., Watanabe S., Giddings, Yamamoto J. (2002) *Thromb. Haemost.* 87, 110-13.
27. Doolitle R.F., Yang Z., Mochalkin Y. (2001) *Ann N Y Acad Sci.* 936, 31-43.
28. Collet J.P, Mishal Z., Vasse M., Mirshani M. Caen J-P., Soria C., Soria J. (1994) *Thrombosis research.* 75, 353-59.

29. Rijken D.C., Hoylaets M., Collen D. (1982) *J.Biol.Chem*. 257, 2920-25.
30. Villanueva J., Canals F., Prat S., Ludevid D., Querol E., Aviles F.X. (1998) *FEBS*. 440, 175-82.
31. Hass M., Derr J., Makus D., Ryan C. (1979) *Plant Physiol*. 64, 1022-28.
32. Villanueva J, Canals F, Villegas V, Querol E, Aviles FX. (2000) *FEBS Lett*. 472, 27-33.
33. Venhudova G, Canals F, Querol E, Aviles FX. (2001) *J. Biol. Chem*. 276, 11683-90.
34. Gonzalez C, Neira JL, Ventura S, Bronsoms S, Rico M, Aviles FX. (2003) *Proteins.* 50, 410-22.
35. Chang JY, Li L, Canals F, Aviles FX. (2000) *J Biol Chem*. 275, 14205-11.
36. Chang JY, Canals F, Schindler P, Querol E, Aviles FX. (1994) *J.Biol.Chem*. 269, 22087-94.

VI. RESUMEN Y DISCUSIÓN GENERAL

El LCI es el primer inhibidor de metalocarboxipeptidasas descrito en sanguijuela y ha sido caracterizado recientemente en nuestro grupo. También hemos desarrollado un sistema de producción recombinante eficiente para dicha molécula (Reverter, 1998) y determinado su estructura tridimensional (Reverter, 2000). Este inhibidor es un polipéptido de 66 aminoácidos cuya estructura está estabilizada por 4 puentes disulfuro (todos ellos localizados entre elementos de estructura secundaria). Esta proteína representa un modelo excelente para el estudio y la mejor comprensión acerca de la diversidad de los caminos de plegamiento de las proteínas pequeñas ricas en puentes disulfuro.

El LCI se comporta como un inhibidor fuerte y competitivo de diferentes tipos de carboxipeptidasas pancreáticas (CPA1, CPA2, CPB) y de la carboxipeptidasa B de plasma (pCPB) con constantes de equilibrio de disociación del orden de $0.1\text{-}0.4\cdot10^{-9}$ M (Reverter, 1998). El valor más bajo entre las K_i del LCI ha sido descrito para la pCPB (carboxipeptidasa B de plasma), un enzima también conocido como TAFI (*Thrombin Activatable Fibrinolysis Inhibitor*), que proteoliza los residuos Lys y Arg C-terminales de la fibrina y regula la activación del plasminógeno, atenuando la fibrinólisis (Wang et al, 1998, Bajzar, 2000). Por ello, el LCI es un excelente candidato para su uso como posible agente fibrinolítico.

VI.A. RESUMEN DE LOS TRABAJOS

En el primer trabajo de esta tesis se dilucida el camino de plegamiento oxidativo del LCI, mediante análisis estructurales y cinéticos de los intermediarios de plegamiento hallados por captura en medio ácido. Se ha observado que el LCI reducido y desnaturalizado se repliega a través de un flujo secuencial y rápido de intermediarios de uno y dos puentes disulfuro, y llega a una etapa limitante en la cual la mezcla de tres especies mayoritarias que contienen 3 puentes disulfuro y una población heterogénea de isómeros de cuatro puentes disulfuro no nativos (*scrambled*) coexisten. Los intermediarios de tres puentes disulfuro se han identificado como trampas cinéticas que se hallan a lo largo del camino de plegamiento del LCI, y se han caracterizado sus estructuras. Los datos obtenidos revelan que dos de ellos contienen sólo puentes disulfuro nativos, y que la tercera trampa cinética contiene un puente nativo y dos no nativos. La coexistencia de tres trampas cinéticas de 3 puentes disulfuro, que adoptan puentes disulfuro nativos, juntamente con una proporción significativa de isómeros *scrambled* totalmente oxidados muestran que el camino de plegamiento del LCI comprende propiedades exhibidas tanto por el BPTI como por la hirudina, dos modelos divergentes con

características de plegamiento opuestas. Los resultados obtenidos en el estudio de las vías de plegamiento del LCI confirman el enorme espectro de diversidad de los caminos de plegamiento de las proteínas.

En el segundo trabajo de esta tesis se dilucidan las curvas de desplegamiento y desnaturalización del LCI, utilizando la técnica del *scrambling* ("mezcla") de disulfuros. En presencia de un agente iniciador de la formación de tioles y un agente desnaturalizante se despliega el LCI nativo por el intercambio de sus puentes disulfuro, y la molécula se transforma en una mezcla de especies *scrambled*. Podemos distinguir claramente y aislar, entre los 104 posibles isómeros *scrambled* del LCI, a nueve de ellos que representan el 90% del total del LCI desplegado. La curva de desnaturalización que muestra la fracción del LCI convertida en isómeros *scrambled* bajo concentraciones crecientes de agentes desnaturalizantes permite deducir que la concentración de tiocianato de guanidinio e hidrocloruro de guanidinio requeridas para alcanzar el 50% de la desnaturalización son de 2,4 y 3,6 M, respectivamente. En contraste, el LCI nativo es resistente a la desnaturalización por urea, incluso a concentraciones elevadas (8M). El camino de desplegamiento del LCI se ha podido definir en base a la evolución de la concentración relativa de los isómeros *scrambled* de la molécula a lo largo de su desnaturalización.

Existen dos poblaciones de especies *scrambled* que sufren variaciones a lo largo del camino de desplegamiento. Una población se acumula como intermediarios bajo condiciones desnaturalizantes fuertes y corresponde a estructuras abiertas o relajadas, entre las cuales se halla el isómero denominado *beads-form*. La otra población muestra una correlación inversa entre su abundancia relativa y las condiciones desnaturalizantes y debería poseer otro tipo de estructuras no nativas, más compactas que el estado desplegado. Las tasas constantes de desplegamiento del LCI resultan bajas al compararse con otras proteínas que contienen puentes disulfuro. Por encima de todo, los resultados que se presentan en el segundo trabajo muestran que el LCI, una molécula con potenciales aplicaciones biotecnológicas, tiene cinéticas bajas de desplegamiento y es altamente estable.

En el tercer trabajo de esta tesis se estudia el efecto del LCI en la fibrinólisis *in vitro*. En la búsqueda de nuevas terapias contra la trombosis, la inhibición de la carboxipeptidasa B de plasma (TAFI) un inhibidor de la fibrinólisis bien conocido, se muestra como una aproximación prometedora. En los últimos años se ha descrito, tanto por estudios *in vitro* como *in vivo*, que el PCI (*potato carboxypeptidase inhibitor*, un inhibidor de carboxipeptidasas de

patata) incrementa la tasa de lisis (mediada por t-PA) de los coágulos de fibrina. Con este mismo propósito, hemos evaluado y comparado la capacidad profibrinolítica del LCI con la del PCI. Todos los resultados han sido obtenidos en ensayos con plasma humano, en un sistema *in vitro*.

Hemos demostrado que ambos inhibidores, el LCI y el PCI, aceleran de forma substancial la lisis de los coágulos tratados con t-PA, esta aceleración es dependiente de la concentración de inhibidor. No obstante el LCI se ha mostrado unas 10 veces más potente que el PCI como acelerador de la fibrinólisis, y también muestra una mayor capacidad inhibidora de TAFI al realizar ensayos de actividad enzimática en plasma. El resultado más prometedor muestra una disminución del tiempo de lisis de 120 a 25 minutos, en concentraciones de 90 nM para el LCI y de 750 nM para el PCI.

También se ha estudiado el posible efecto de estos dos inhibidores sobre la estructura del coágulo de fibrina mediante microscopía electrónica de transmisión y de barrido. Al inducir la coagulación del plasma humano en presencia de LCI y de PCI se ha observado un incremento significativo en el grosor de las fibras y una disminución simultánea en la densidad de su entrecruzamiento. Estas alteraciones en la estructura del coágulo se correlacionan con la tasa de fibrinólisis que hemos calculado a partir de los datos turbidimétricos. Todos estos resultados sugieren que el LCI puede tener una aplicación en las terapias trombolíticas basadas en t-PA.

VI.B. DISCUSIÓN GENERAL

VI.B.1. El plegamiento del LCI

Los mecanismos de plegamiento oxidativo de las proteínas pequeñas ricas en puentes disulfuro estudiados hasta hoy en día varían significativamente de unos a otros (Creighton, 1978, Creighton & Goldenberg, 1984, Weissman & Kim, 1991, Goldenberg, 1992, Chang, 1994). Podemos describir estas diferencias en base a los casos paradigmáticos del BPTI (Weissman & Kim, 1991) y la hirudina (Chatrenet & Chang, 1993, Chang, 1994), cada uno de los cuales representa un conjunto de proteínas con características de plegamiento similares. Las diferencias en sus vías de plegamiento vienen ilustradas por:

-La homogeneidad (BPTI) versus la heterogeneidad (hirudina) en los intermediarios de plegamiento.

-La predominancia (BPTI) versus la inexistencia (hirudina) de intermediarios con puentes disulfuro nativos.
-La ausencia (BPTI) versus la presencia (hirudina) de isómeros *scrambled* totalmente oxidados como intermediarios de plegamiento.

Brevemente, para el BPTI el camino de plegamiento pasa a través de unas pocas formas, mayoritarias, de intermediarios de plegamiento que adoptan puentes disulfuro y estructuras parecidas a la nativa. Para la hirudina, el plegamiento aparentemente procede a través de un estado inicial de formación no específica de disulfuros (empaquetamiento), seguido de una reorganización de disulfuros de los intermediarios *scrambled* heterogéneos (consolidación), para asumir la estructura nativa.

El mecanismo del plegamiento oxidativo del LCI, dilucidado en el primer trabajo de la presente tesis, comprende rasgos de ambos modelos: el del BPTI y el de la hirudina. Al igual que en la hirudina se observa un flujo de intermediarios altamente heterogéneos de uno y dos puentes disulfuro en las fases tempranas del plegamiento; estos intermediarios dan paso, rápidamente, a dos poblaciones distintas. Una población consiste en una mezcla compleja de especies *scrambled* de 4 puentes disulfuro, incapaces de evolucionar efectivamente hacia la estructura nativa a menos que se encuentre en el medio un catalizador de la formación de tioles. La otra población comprende tres isómeros predominantes de 3 puentes disulfuro. Entre ellos, dos contienen exclusivamente puentes disulfuro nativos. Al igual que en el caso del BPTI dichos intermediarios son estables y representan una etapa limitante en el plegamiento de la proteína que nosostros hemos identificado como trampas cinéticas, dado que ninguno de estos intermediarios evoluciona fácilmente hacia la forma nativa.

En este primer trabajo también se describe que la eficiencia del plegamiento oxidativo (tasa de recuperación de la proteína nativa) del LCI depende de los agentes redox incluidos en el medio. La cinética de formación de puentes disulfuro se ve acelerada por el GSSG, mientras que la cinética del reordenamiento de disulfuros requiere tioles libres (GSH o β-mercaptoetanol) en el medio. De todos modos, la población y el patrón de los intermediarios de plegamiento del LCI permanece fundamentalmente invariable, a pesar de la presencia de agentes redox. Este efecto único del sistema redox GSSG/GSH en el mecanismo de plegamiento oxidativo se ha demostrado igualmente para un gran número de proteínas pequeñas ricas en puentes disulfuro, incluyendo la hirudina (Chang, 1994), el PCI (Chang et al, 1994), el TAP (Chang, 1996) y la α-lactalbúmina (Chang & Li, 2002), entre otras.

A partir de los patrones de HPLC obtenidos a tiempo variable en el proceso de plegamiento, podemos observar cómo los intermediarios de plegamiento del LCI se

distribuyen ampliamente entre la especie nativa y la completamente reducida. Las fracciones que contienen uno o dos puentes disulfuro se hallan localizadas cerca del LCI completamente desplegado y lejos del LCI nativo, mientras que tanto los *scrambled* (de cuatro disulfuros) como las trampas cinéticas de 3 puentes disulfuro se hallan relativamente más cercanos a la fracción de la proteína nativa.

Por tanto, existe una gran diferencia de hidrofobicidad entre las especies de 1 y 2 disulfuros y los *scrambleds* y trampas cinéticas. A partir del gradiente utilizado en la cromatografía de fase reversa, se puede deducir que el LCI nativo posee la estructura menos hidrofóbica y que correspondería al mínimo de energía entre todas las isoformas posibles de la proteína, ya que es una estructura globular compacta. En el otro extremo, el LCI completamente reducido posee la mayor hidrofobicidad, y presumiblemente sea la estructura más abierta y relajada. Siguiendo estos principios, los isómeros *scrambled* y el intermediario III-B (de tres puentes disulfuro) deben compartir un grado similar de hidrofobicidad y compactación, puesto que se hallan todos localizados en la misma fracción. Los intermediarios III-A1 y III-A2 poseen menor hidrofobicidad, y presuntamente un mayor grado de empaquetamiento. Presumiblemente, todos estos intermediarios, los *scrambleds* y las trampas cinéticas, tengan un grado similar y elevado de compactación (a pesar de la heterogeneidad de la fracción de *scrambleds*) puesto que pueden representar mínimos locales de la energía libre en el camino de plegamiento de la proteína, explicando entonces la necesidad de añadir tioles adicionales o promotores de puentes disulfuro para obtener una recuperación completa del LCI.

Es probable, pues, que para transformar los intermediarios de tres puentes disulfuro en la forma nativa, se requieran cambios conformacionales posteriores y no se descarta la posibilidad ni de que existan reorganizaciones estructurales que mantengan los puentes disulfuro ya formados ni de que se produzcan reordenamientos posteriores de los disulfuros hacia una población más productiva y tal vez más heterogénea de *scrambleds*.

La conversión de los intermediarios de 3 puentes disulfuro y los isómeros de 4 puentes disulfuro en proteína nativa sucede simultáneamente, y contemplamos ambas poblaciones como un paso limitante en la recuperación de la proteína. Se hacen obvias entonces la pluralidad y complejidad del camino de plegamiento del LCI, lo que concuerda con la ausencia de una única vía de plegamiento en los casos de las proteínas de cuatro puentes disulfuro estudiadas hasta hoy día. El LCI, la ribonucleasa A y la α-lactalbúmina presentan modelos que dan apoyo a la idea comúnmente extendida de que para la mayoría de las proteínas no existe una única vía de plegamiento específica, sino que se pueden trazar un número

determinado de rutas simultáneas dibujando así un paisaje energético (ilustrado por el embudo de plegamiento). La naturaleza, el tamaño y los dominios estructurales de las proteínas determinaran la complejidad y lo abrupto de este paisaje energético, encontrándonos en el presente caso del LCI con tres mínimos locales de energía libre que entendemos como trampas cinéticas.

En el caso de las proteínas pequeñas ricas en puentes disulfuro los procesos de oxidación y reducción de sus puentes disulfuro nativos se hallan correlacionados, en general, con los procesos de plegamiento y desplegamiento de la proteína respectivamente (Anfinsen, 1973). Por ello es necesario atrapar y caracterizar químicamente a los intermediarios de ambos procesos.

En el caso de la caracterización de las vías de desplegamiento de diversas proteínas es extremadamente útil la observación de que en presencia de cantidades traza de un agente iniciador de la formación de tioles durante el desplegamiento por agentes desnaturalizantes se genera una mezcla de intermediarios que consisten mayoritariamente en isómeros *scrambled* con disulfuros no-nativos que aún mantienen el número nativo de puentes disulfuro. A partir de ello, se ha descrito una nueva metodología (Chang, 1997) que ha permitido determinar la estabilidad frente a desnaturalizantes y dilucidar el camino de desplegamiento de diversas proteínas como el TAP (Chang, 1999), el ILGF (Chang et al, 1999) y el PCI (Chang et al, 2000).

Esta metodología se utiliza en el segundo trabajo de la presente tesis para describir el camino de desplegamiento y la estabilidad conformacional del LCI mediante la caracterización de las especies *scrambled* generadas en presencia de un agente iniciador de la formación de tioles. De los 104 posibles isómeros *scrambled* para el LCI en su vía de desplegamiento, hemos detectado claramente la existencia de nueve de ellos. A estos intermediarios se los puede dividir en dos poblaciones según las variaciones de concentración que sufren a lo largo del camino de desplegamiento. Una población se acumula bajo condiciones desnaturalizantes fuertes (X-LCI-a, X-LCI-b) y por los estudios realizados en otras proteínas (Chang, 1999, Chang et al, 1999, Chang et al, 2000) se espera que posea estructuras abiertas o relajadas. Esta hipótesis toma fuerza por la constatación de que el isómero X-LCI-a es el intermediario *beads-form* (aquel que posee sus cisteínas apareadas correlativamente, en una de las estructuras probablemente más relajadas que puedan hallarse). La segunda población (X-LCI-f, X-LCI-h, X-LCI-g), en contraste, muestra una correlación inversa entre sus abundancias relativas y la concentración de agentes desnaturalizantes. Esta población debería tener otro tipo de

estructura, probablemente más compacta que el estado desplegado, que fuese inestable a elevadas concentraciones de desnaturalizantes.

También en el segundo trabajo se ha caracterizado la estabilidad conformacional del LCI. Para estudiarla, hemos trazado sus curvas de desnaturalización: bajo concentraciones crecientes de un agente desnaturalizante determinado se representa la fracción del LCI nativo convertido en especies *scrambled*. Según las curvas obtenidas, el cloruro de guanidinio y el cloruro de tiocianato desnaturalizan al LCI de forma cooperativa a concentraciones entre 2-3 y 3-4 M, respectivamente. Estos valores son más elevados que para el PCI, otro inhibidor de carboxipeptidasas sin apenas estructura secundaria (Rees & Lipscomb, 1982, Clore et al, 1987) que, aunque muestra una menor estabilidad que el LCI, todavía es una proteína muy estable al mantenerse su estructura globular por la formación de un núcleo hidrofóbico compacto y presentar una estructura en T-knot (dos puentes disulfuro atravesados por un tercero, estructura hallada en muchas y diversas proteínas). Entonces, la concentración más elevada de desnaturalizantes que se requiere para el LCI podría reflejar la contribución de la estructura secundaria a la estabilidad del plegamiento del LCI, hecho que también refleja el cambio abrupto entre 6 y 7 M de cloruro de guanidinio, indicativo de la naturaleza cooperativa del proceso y de la relevancia de los puentes de hidrógeno (básicos en el mantenimiento de la estructura secundaria) en el mismo. El hecho de que la urea no sea capaz de desnaturalizar al LCI, pero sí lo sea el cloruro de guanidinio se explica asimismo por la interacción de ambos agentes con las fuerzas hidrofóbicas que mantienen la estructura de las proteínas. Ambos desnaturalizantes entorpecen las interacciones no covalentes que estabilizan el plegamiento nativo (Dill & Shortle, 1991), principalmente las interacciones hidrofóbicas, haciendo que el agua sea un mejor solvente para los aminoácidos no polares. Además, el cloruro de guanidinio es también una sal y por tanto suprime las interacciones electrostáticas, que son fundamentales para mantener la estructura de una proteína con un plegamiento totalmente en forma de láminas-β, que es prácticamente el caso del *core* del LCI. De ahí que, la urea, al no entorpecer estas interacciones electrostáticas (de nuevo reflejo de los puentes de hidrógeno formados en la estructura secundaria) sea incapaz de desnaturalizar al LCI.

Cabe también destacar que el LCI es globalmente la proteína más estable estudiada por el método descrito, puesto que ni la inclusión en el medio de un 65% de metanol, ni el tratamiento a elevadas temperaturas (65ºC, una hora) pueden desnaturalizarlo. La elevada estabilidad del LCI surge de una combinación óptima de puentes disulfuro, un *core* hidrofóbico compacto y un porcentaje elevado de estructura secundaria regular. Esta elevada estabilidad hace que la molécula sea una candidata óptima a aplicaciones en terapias biomédicas y, en este

contexto, el conocimiento de la estabilidad y el comportamiento del plegamiento del LCI constituye una base para el desarrollo de variantes de la molécula con actividad y estabilidad mejorada.

VI.B.2. El efecto fibrinolítico del LCI

Uno de los principales problemas que comparten todas las terapias trombolíticas que se utilizan en la actualidad es la resistencia de los trombos a su degradación por el fármaco que se esté administrando para tal fin. Al aumentar la dosis de dicho agente trombolítico este problema desaparece, pero entonces se corre el peligro de que entren en escena diversos efectos secundarios entorpeciendo el correcto funcionamiento de varios factores de la cadena de coagulación y pudiendo terminar con cuadros críticos de hemorragias internas (Neuhaus et al, 1994, Refino et al, 2000). El más común de los fármacos administrados en tratamientos trombolíticos de choque es el t-PA (activador tisular del plasminógeno).

Las nuevas terapias que se están desarrollando en la actualidad van encaradas a minimizar ambos problemas. Se ha demostrado recientemente, en diversos modelos tanto *in vitro* como *in vivo,* que el tratamiento con t-PA al administrar conjuntamente un inhibidor selectivo de TAFI incrementa su eficacia (se requieren dosis menores para conseguir el mismo efecto) y se eliminan los riesgos colaterales de sangrado. Los inhibidores que se han utilizado hasta hoy día han sido el argatroban, un inhibidor sintético con el que se han realizado estudios en ratas (Hashimoto et al, 2002), y el PCI, del que hablamos a continuación.

EL PCI es un inhibidor de metalocarboxipeptidasas que se halla en la patata y para el que existen homólogos en otras *solanacea* como el tomate o la calabaza. El PCI se ha usado con frecuencia en los estudios concernientes a la caracterización de la actividad y modo de actuación de TAFI, dada su capacidad de inhibir específicamente TAFI pero no a la CPN. Aparte de TAFI, el PCI inhibe un amplio abanico de carboxipeptidasas del tracto digestivo, y carboxipeptidasas microbianas.

Así pues, diversos estudios han presentado pruebas convincentes de un posible rol del PCI en terapias trombolíticas *in vivo*, en modelos de trombosis arterial y trombosis venosa en conejos (Klement et al, 1998, Klement et al, 1999, Nagashima et al, 2000). La especificidad del PCI le permite actuar sin afectar a la presión y coagulación sanguínea ni a las concentraciones de fibrinógeno, principales efectos secundarios de las sobredosis por t-PA. Así pues, vemos como el PCI se ha usado en un determinado número de estudios *in vivo* como un inhibidor de TAFIa con resultados bastante esperanzadores lo que hace prever que su uso se incremente en un futuro próximo dada la necesidad de hallar nuevas opciones a las terapias tradicionales.

En el tercer trabajo de la presente tesis aportamos una nueva alternativa para el desarrollo de las terapias trombolíticas basadas en la inhibición de TAFI con el LCI, el inhibidor de carboxipeptidasas de sanguijuela.

En este trabajo se presentan evidencias experimentales de que el tratamiento de plasma humano (estudios *in vitro*) con LCI recombinante provoca una inhibición completa de la actividad de TAFI y aumenta significativamente la actividad trombolítica del t-PA. Según nuestros resultados, tanto de los ensayos de medición de la velocidad de fibrinólisis como de los ensayos acerca de la inhibición de la actividad enzimática de TAFI en plasma, se extrae que el LCI es aproximadamente unas 10 veces más efectivo que el PCI, dadas las concentraciones necesarias de ambos inhibidores para obtener un mismo efecto. Dada la correlación entre los resultados de los ensayos de coagulación y los ensayos de actividad enzimática realizados en plasma, se demuestra que la aceleración de la fibrinólisis por el LCI es efecto directo de su inhibición de la actividad enzimática de TAFI y, en principio, se descarta la posibilidad de que dicha aceleración sea consecuencia de otros efectos laterales sobre diversos componentes del sistema hemostásico.

Enfocando el problema desde otro punto de vista, es bien conocido que la susceptibilidad de los coágulos a su degradación por plasmina depende de cómo esté organizada la red de fibrina que forma el coágulo. Un cambio en las condiciones de polimerización que llevan al ensamblaje no covalente de los monómeros podría afectar a la estructura de las protofibrillas. En el tercer trabajo de la presente tesis se ha puesto en marcha un diseño experimental que nos permite observar el efecto de la actividad de TAFI sobre la estructura de la malla de fibrina. Sospechábamos que, tal vez, la ruptura de los residuos lisina y arginina C-terminales de la superficie del fibrinógeno, llevada a cabo por TAFI, podría interferir con la agregación lateral de las fibras y afectar a la estructura final del coágulo, lo que proporcionaría una explicación morfológica a la resistencia de los coágulos a la lisis en condiciones de elevada actividad TAFI. Hemos emulados dos casos extremos en el plasma: una elevada actividad de TAFI, que se consigue aumentando la dosis de TR-TM y una ausencia total de la actividad de TAFI, que se consigue a concentraciones saturantes de inhibidor (LCI o PCI), lo cual nos permite, además, observar un posible efecto de interferencia de los inhibidores con la estructura de fibrina. En ambos casos se observó la formación y lisis del coágulo, mediante microscopía electrónica de *scanning* (“rastreo”) (MES).
Los resultados que hemos obtenidos por MES muestran como una elevada actividad TAFI provoca la formación de mallas de fibrina de fibras delgadas y tamaños de poro irregulares y pequeños, dando la sensación de apelmazamiento del coágulo. Por el contrario, la morfología

observada en presencia de concentraciones saturantes de PCI o LCI muestra unos coágulos formados por fibras más gruesas y poros más grandes, dando en conjunto la sensación de una red más organizada y esponjosa, donde los elementos de la cadena fibrinolítica pueden difundir mejor.

Aunque desconocemos el mecanismo por el cual TAFI puede afectar a la estructura de las protofibrillas pensamos que la eliminación de los LBS (lugares de unión a lisina) de la fibrina parcialmente degradada podría, tal vez, afectar el grosor de las fibras y ser la responsable de los cambios morfológicos observados.

Estos cambios morfológicos son consistentes con el efecto del retraso fibrinolítico de TAFI, dados los numerosos estudios que demuestran que a mayor grosor de las fibras, mayor es la tasa de absorción del t-PA, y, por tanto, mayor la velocidad de fibrinólisis (Bajzar et al, 1996). Así pues, según nuestras observaciones, una elevada actividad de TAFI conlleva un menor grosor en las fibras y por tanto una menor tasa de fibrinólisis. Lo contrario sucede a elevadas concentraciones de LCI o PCI.

Los análisis realizados por MET (microscopía electrónica de transmisión) confirman los resultados obtenidos por MES, aunque no aportan información acerca de posibles variaciones en la subestructura de las protofibrillas por la actividad de TAFI. En nuestras micrografías no se observan alteraciones en el ensamblaje de los monómeros de fibrina, aunque en algún punto entre la dimerización y la agregación lateral debe existir alguna alteración, puesto que se observan diferencias en la ramificación de las fibras. Debemos remarcar que el ensayo de MET no es más que un estudio preliminar, y necesitaríamos un mayor número de estudios para poder discernir el mecanismo por el cual TAFI afecta a la estructura del coágulo.

En resumen, los datos obtenidos en el presente trabajo muestran la capacidad del LCI de inhibir fuertemente TAFI en plasma humano y, a través de esta acción, acelerar significativamente el mecanismo de la fibrinólisis y la degradación de la estructura del coágulo. Este trabajo, pues, da soporte a la hipótesis de que el LCI puede ser un buen coadyuvante en las terapias trombolíticas mediadas por t-PA. Como hemos citado, el inhibidor con el que se han realizado el mayor número de estudios hasta hoy día es el PCI. Dada la importancia de la necesidad de hallar nuevos enfoques terapéuticos y previniendo la aparición en un futuro próximo de un mayor número de estudios, es importante constatar que el PCI puede tener efectos adicionales en un modelo *in vivo*. Aunque el papel biológico del PCI no está demostrado, probablemente se halla involucrado en la defensa de las plantas contra plagas. No se han hallado efectos de toxicidad del PCI en ratones, y su vida media en conejos está

estimada en unos 10 minutos. Ahora bien, podemos aventurar aquí que el LCI, aparte de ser un mejor inhibidor de TAFI y un profibrinolítico más eficaz que el PCI, como acabamos de demostrar, puede ser una molécula potencialmente apropiada para uso terapéutico interno en humanos. El LCI proviene de las sanguijuelas, un parásito que se alimenta de sangre de mamíferos. Las sanguijuelas tienen la necesidad de generar perturbaciones locales mínimas en el huésped después de la mordedura, lo que conlleva a una adaptación inmunológica y toxicológica de las moléculas del invasor que estén en contacto con el punto de sangrado. Aunque, nuevamente, la funcionalidad biológica del LCI no está demostrada, el hecho de que sus dianas deben hallarse en el torrente sanguíneo de mamíferos augura, en nuestra opinión, un futuro más esperanzador que el del PCI en el desarrollo de nuevos fármacos coadyuvantes para las terapias trombolíticas.

VII. CONCLUSIONES

De los estudios de plegamiento que componen la primera parte de esta tesis se extraen las siguientes conclusiones:

1. El LCI reducido y desnaturalizado se repliega a través de un flujo rápido y secuencial de intermediarios de uno y dos puentes disulfuro, llegando a una etapa limitante en la que coexisten una población heterogénea de intermediarios *scrambled* totalmente oxidados y tres intermediarios de tres puentes disulfuro identificados como trampas cinéticas. Dos de los tres intermediarios poseen todos sus puentes disulfuro nativos.
2. El camino de plegamiento del LCI comparte rasgos tanto del BPTI como de la hirudina, dos modelos muy divergentes de plegamiento. Para el LCI no existe una única vía de plegamiento, sino que sus rutas simultáneas dibujan un paisaje energético que ilustra la idea cada vez más aceptada de "embudo de plegamiento".
3. El LCI, en presencia de un agente iniciador de la formación de tioles y un agente desnaturalizante, se despliega dando lugar a una población heterogénea de isómeros *scrambled*. De los 104 posibles isómeros aparecen como claramente identificables nueve de ellos y se observan dos poblaciones de comportamientos contrarios: una de ellas se acumula, mientras que la otra desaparece, bajo condiciones desnaturalizantes fuertes.
4. El LCI posee cinéticas bajas de desplegamiento y es la proteína de mayor estabilidad conformacional de las estudiadas hasta hoy día por la técnica del *scrambling* de disulfuros.
5. Los estudios de estabilidad y plegamiento del LCI constituyen la base para hallr variantes más estables y activas de la molécula con la perspectiva de su potencial aplicación biomédica.

De los estudios de la funcionalidad biológica del LCI que componen la segunda parte de esta tesis se extraen las siguientes conclusiones:

1. La adición de LCI en plasma con retraso fibrinolítico debido a una elevada actividad de TAFI provoca la aceleración de la velocidad de fibrinólisis, de manera dependiente de la concentración añadida. En consecuencia, concluímos que el LCI es un buen fibrinolítico *in vitro*.
2. El LCI inhibe la actividad carboxipeptidasa de TAFI en plasma, de forma que se correlacionan las dosis requeridas para un determinado efecto profibrinolítico con las dosis necesarias para inhibir al enzima. Por tanto, el efecto fibrinolítico del LCI se debe a su actividad inhibidora de TAFI.

3. La concentración requerida de LCI para conseguir un mismo efecto sobre la fibrinólisis que con el PCI es aproximadamente 10 veces menor. Igualmente, esta correlación se mantiene en las detecciones de actividad inihibodora de TAFI en plasma. Por lo tanto, se deduce que, *in vitro*, el LCI es un profibrinolítico más potente que el PCI.
4. La red de fibrina que conforma los coágulos queda morfológicamente afectada por la actividad de TAFI. Confirmamos visualmente la correlación entre la inhibición de TAFI por LCI o PCI, la aceleración de la fibrinólisis y los cambios en las mallas de fibrina de los coágulos.

VIII. BIBLIOGRAFÍA GENERAL

A

Anfinsen CB. Principles that govern the folding of protein chains. *Science.* 1973. 181: 223-30.

B

Bajzar L, Fredenburgh JF, Nesheim M. The activated protein C-mediated enhancement of tissue-type plasminogen activator-induced fibrinolysis in a cell-free system. *J Biol Chem*. 1990. 265: 16948–16954.

Bajzar L, Nesheim M. The effect of activated protein C on fibrinolysis in cell-free plasma can be attributed specifically to attenuation of prothrombin activation. *J Biol Chem*. 1993. 268: 8608–8616.

Bajzar L, Manuel R, Nesheim ME. Purification and characterization of TAFI, a thrombin-activatable fibrinolysis inhibitor. *J Biol Chem*. 1995. 270: 14477–14484.

Bajzar L, Nesheim ME, Tracy PB. The profibrinolytic effect of activated protein C in clots formed from plasma is TAFI-dependent. *Blood*. 1996. 88: 2093–2100.

Bajzar L, Morser J, Nesheim M. TAFI, or plasma procarboxypeptidase B, couples the coagulation and fibrinolytic cascades through the thrombin–thrombomodulin complex. *J Biol Chem.* 1996. 271: 16603–16608

Bajzar L, Taylor F, Tracy PB. A baboon model can be used to assess the physiologic function of TAFI. *Thromb Haemostasis*. 1997. Suppl. 1: 596.

Bajzar L. Thrombin activatable fibrinolysis inhibitor and an antifibrinolytic pathway. *Arterioscler Thromb Vasc Biol*. 2000. 20: 2511-8.

Boffa MB, Wang W, Bajzar L, Nesheim ME. Plasma and recombinant thrombin-activable fibrinolysis inhibitor (TAFI) and activated TAFI compared with respect to glycosylation, thrombin/thrombomodulin-dependent activation, thermal stability, and enzymatic properties. *J Biol Chem*. 1998. 273: 2127–2135.

Boffa MB, Bell R, Stevens WK, Nesheim ME. Roles of thermal instability and proteolytic cleavage in regulation of activated thrombin-activable fibrinolysis inhibitor. *J Biol Chem*. 2000. 275: 12868–12878.

Bouma B, Von dem Borne P, Meijers J. Factor XI and protection of the fibrin clot against lysis: a role for the intrinsic pathway of coagulation in fibrinolysis. *Thromb Haemostasis*. 1998. 80: 24–27.

Bouma B, Mosnier L, Meijers JMC and Griffin JH. Factor XI dependent and independent activation of thrombin-activatable fibrinolysis inhibitor (TAFI) in plasma associated with clot formation. *Thromb Haemostasis*. 1999. 82: 1703–1708.

Bulychev A, Chang JY. Unfolding of hirudin characterized by the composition of denatured scrambled isomers. *J Protein Chem.* 1999. 18: 771-8.

Burgos FJ, Salva M, Villegas M, Soriano M, Mendez E, Avilés FX. Analysis of the activation process of porcine procarboxypeptidase B and determination of the sequence of its activation segment. *Biochemistry*. 1991. 30: 4082–4089.

C

Campbell W, Okada H. An arginine specific carboxypeptidase generated in blood during coagulation or inflammation which is unrelated to carboxypeptidase N or its subunits. *Biochem Biophys Res*. 1989. 162: 933–939.

Chang JY. Controlling the speed of hirudin folding. *Biochem J*. 1994. 300: 643-50.

Chang JY, Canals F, Schindler P, Querol E, Aviles FX. The disulfide folding pathway of potato carboxypeptidase inhibitor. *J Biol Chem*. 1994. 269: 22087-94.

Chang JY, Schindler P, Ramseier U, Lai PH. The disulfide folding pathway of human epidermal growth factor. *J Biol Chem*. 1995. 270: 9207-16.

Chang JY. The disulfide folding pathway of tick anticoagulant peptide (TAP), a Kunitz-type inhibitor structurally homologous to BPTI. *Biochemistry*. 1996. 35: 11702-9.

Chang JY, Marki W, Lai PH. Analysis of the extent of unfolding of denatured insulin-like growth factor. *Protein Sci.* 1999. 8:1463-8.

Chang JY. Denatured states of tick anticoagulant peptide. Compositional analysis of unfolded scrambled isomers. *J Biol Chem*. 1999. 274: 123-8.

Chang JY, Ballatore A. Structure and heterogeneity of the one- and two-disulfide folding intermediates of tick anticoagulant peptide. *J Protein Chem*. 2000. 19: 299-310.

Chang JY, Li L, Bulychev A. The underlying mechanism for the diversity of disulfide folding pathways. *J Biol Chem*. 2000. 275: 8287-9.

Chang JY, Li L, Canals F, Aviles FX. The unfolding pathway and conformational stability of potato carboxypeptidase inhibitor. *J Biol Chem*. 2000. 275: 14205-11.

Chang JY, Li L. The structure of denatured alpha-lactalbumin elucidated by the technique of disulfide scrambling: fractionation of conformational isomers of alpha-lactalbumin. *J Biol Chem*. 2001. 276: 9705-12.

Chang JY, Li L, Lai PH. A major kinetic trap for the oxidative folding of human epidermal growth factor. *J Biol Chem*. 2001. 276: 4845-52.

Chang JY, Li L. Pathway of oxidative folding of alpha-lactalbumin: a model for illustrating the diversity of disulfide folding pathways. *Biochemistry*. 2002. 41: 8405-13.

Chang JY. The folding pathway of alpha-lactalbumin elucidated by the technique of disulfide scrambling. Isolation of on-pathway and off-pathway intermediates. *J Biol Chem*. 2002. 277: 120-6.

Chatrenet B, Chang JY. The disulfide folding pathway of hirudin elucidated by stop/go folding experiments. *J Biol Chem*. 1993. 268: 20988-96.

Chetaille P, Alessi MC, Kouassi D, Morange PE Juhan-Vague I. Plasma TAFI antigen variations in healthy subjects. *Thromb Haemostasis*. 2000. 83: 902–905.

Clore GM, Gronenborn AM, Nilges M, Ryan CA. Three-dimensional structure of potato carboxypeptidase inhibitor in solution. A study using nuclear magnetic resonance, distance geometry, and restrained molecular dynamics. *Biochemistry*. 1987. 26: 8012-23.

Creighton TE. Experimental studies of protein folding and unfolding. *Prog Biophys Mol Biol*. 1978. 33: 231-97.

Creighton TE. The single-disulphide intermediates in the refolding of reduced pancreatic trypsin inhibitor. *J Mol Biol*. 1974. 87: 603-24.

Creighton TE. Related The two-disulphide intermediates and the folding pathway of reduced pancreatic trypsin inhibitor. *J Mol Biol*. 1975. 95: 167-99.

Creighton TE. Related Energetics of folding and unfolding of pancreatic trypsin inhibitor. *J Mol Biol*. 1977. 113: 295-312.

Creighton TE. Related Role of the environment in the refolding of reduced pancreatic trypsin inhibitor. *J Mol Biol*. 1980. 144: 521-50.

Creighton TE, Goldenberg DP. Folding pathway of a circular form of bovine pancreatic trypsin inhibitor. *J Mol Biol*. 1984. 179: 527-45.

Creighton TE. Disulfide bonds as probes of protein folding pathways. *Methods Enzymol*. 1986. 131: 83-106.

Creighton TE. Related Protein folding. *Biochem J*. 1990. 270: 1-16.

D

Dill KA. Theory for the folding and stability of globular proteins. *Biochemistry*. 1985. 24: 1501-9.

Dill KA, Shortle D. Denatured states of proteins. *Annu Rev Biochem*. 1991. 60: 795-825.

Dill KA, Chan HS. From Levinthal paradox to pathways to funnel. *Nature Struct Biol*. 1997. 4: 10-19.

Dobrovolsky AB, Titaeva EV. The fibrinolysis system: regulation of activity and physiologic functions of its main components. *Biochemistry*. 2002. 67: 99-108.

Dobson CM, Sali A, Karplus M. Protein folding: A perspective from theory and experiment. *Angewandte Chemie*. 1998. 37: 868-893.

E

Eaton DL, Malloy BE, Tsai SP, Henzel W, Drayna D. Isolation, molecular cloning, and partial characterization of a novel carboxypeptidase B from human plasma. *J Biol Chem*. 1991. 266: 21833–21838.

Ellis RJ, Hartl FU. Principles of protein folding in the cellular environment. *Curr Opin Struct Biol*. 1999. 9: 102-10.

Erdös EG, Sloane EM. An enzyme in human blood plasma that inactivates bradykinin and kallidins. *Biochem Pharmacol*. 1962. 11: 585–592.

Erdös EG, Renfrew AG, Sloane AM, Wohler JR. *Ann N Y Acad Sci*. 1963. 104: 234.

Ewbank JJ, Creighton TE. Pathway of disulfide-coupled unfolding and refolding of bovine alpha-lactalbumin. *Biochemistry*. 1993. 32: 3677-93.

F

Fersht AR. Related Nucleation mechanisms in protein folding. *Curr Opin Struct Biol*. 1997. 7: 3-9.

Fink A.L. Compact intermediate states in protein folding. *Annual Review of Biophysics and Biomolecular Structure*. 24: 495-522.

De Fouw NJ, Haverkate F, Bertina RM. Protein C and fibrinolysis: a link between coagulation and fibrinolysis. *Adv Exp Med Biol*. 1990. 281: 235–243.

G

Gaffney PJ. Fibrin degradation products. A review of structures found in vitro and in vivo. *Ann N Y Acad Sci*. 2001. 936: 594-610.

Goldenberg DP. Native and non-native intermediates in the BPTI folding pathway. *Trends Biochem Sci*. 1992. 17: 257-61.

Griffin JH. Blood coagulation: the thrombin paradox. *Nature*. 1995. 378: 337–338.

H

Hashimoto M, Yamashita T, Oiwa K, Watanabe S, Giddings JC, Yamamoto J. Enhancement of endogenous plasminogen activator-induced thrombolysis by argatroban and APC and its control by TAFI, measured in an arterial thrombolysis model in vivo using rat mesenteric arterioles. *Thromb Haemost*. 2002. 87: 110-3.

Hendriks D, Scharpé S, van Sande M, Lommaert MP. A labile enzyme in fresh human serum interferes with the assay of carboxypeptidase N. *Clin Chem*. 1989. 35: 177-183.

Hendriks D, Scharpé S, van Sande M, Lommaert MP. Characterisation of a carboxypeptidase in human serum distinct from carboxypeptidase N. *J Clin Chem Clin Biochem*. 1989. 27: 277–285.

Hendriks D, Wang W, Scharpé S, Lommaert MP, van Sande M. Purification and characterization of a new arginine carboxypeptidase in human serum. *Biochim Biophys Acta*. 1990. 1034: 86–92.

Hori Y, Gabazza EC, Yano Y, Katsuki A, Suzuki K, Adachi Y, Sumida Y. Insulin resitance is asociated with an increased circulating level of thrombin activatable fibrinolysis inhibitor in type 2 diabetes pacients. *J.Clin Endocrinol Metab*. 2002. 87: 2.

J

Jaenicke R. Folding and association of proteins. *Prog Biophys Mol Biol*. 1987. 49: 117-237.

Jeng MF, Englander SW. Stable submolecular folding units in a non-compact form of cytochrome c. *J Mol Biol*. 1991. 221: 1045-61.

K

Karplus M, Sali A. Theoretical studies of protein folding and unfolding. *Curr Opin Struct Biol*. 1995. 5: 58-73.

Karplus M, Weaver DL. Protein folding dynamics: the diffusion-collision model and experimental data. *Protein Sci*. 1994. 3: 650-68.

Kim PS, Baldwin RL. Intermediates in the folding reactions of small proteins. *Annu Rev Biochem*. 1990. 59: 631-60.

Klement P, Liao P, Bajzar L. An inhibitor of activated TAFI enhances thrombolysis in vivo. *Blood*. 1998. 92 (Suppl 1): 709a.

Klement P, Liao P, Bajzar L. A novel approach to arterial thrombolysis. *Blood*. 1999. 94: 2735–2743.

Kokame K, Zheng XL, Sadler JE. Activation of thrombin-activable fibrinolysis

inhibitor requires epidermal growth factor-like domain 3 of thrombomodulin and is inhibited competitively by protein C. *J Biol Chem.* 1998. 273: 12135–12139.

L

Levinthal C. Are there pathways for protein folding? *J Cim Phys.* 1968. 65: 44-45

Lim-Wilby MS, Hallenga K, de Maeyer M, Lasters I, Vlasuk GP, Brunck TK. NMR structure determination of tick anticoagulant peptide (TAP). *Protein Sci*. 1995. 4: 178-86.

M

Mao SS, Cooper CM, Wood T, Shafer JA, Gardell SJ. Characterization of plasmin-mediated activation of plasma procarboxypeptidase B, modulation by glycosaminoglycans. *J Biol Chem.* 1999. 274: 35046–35052.

Marlar RA, Kleiss AJ, Griffin JH. An alternative extrinsic pathway of human blood coagulation. *Blood.* 1982. 60 1353–1358.

Marx PF, Wagenaar G, Reijerkerk A, Tiekstra MJ, Van Rossum AG, Gebbink MF, Meijers MC. Characterization of mouse thrombin-activatable fibrinolysis inhibitor. *Thromb Haemostasis.* 2000. 83: 297–303.

Matouschek A, Fersht AR. Protein engineering in analysis of protein folding pathways and stability. *Methods Enzymol*. 1991. 202: 82-112.

Meijers J, Middeldorp S, Tekelenburg W, Van den Ende AE, Tans G, Prins MH, Rosing J, Büller R, Bouma BN. Increased fibrinolytic activity during use of oral contraceptives is counteracted by an enhanced factor XI-independent downregulation of fibrinolysis — a randomized cross-over study of two low-dose oral contraceptives. *Thromb Haemostasis.* 2000. 84: 9–14

Meijers J, Oudijk EJD, Mosnier LO, Bos R, Bouma BN, Nieuwenhuis HK, Fijnheer R. Reduced activity of TAFI (thrombin-activatable fibrinolysis inhibitor) in acute promyelocytic leukaemia. *Br J Haematol*. 2000. 108: 518–523

van Mierlo CP, Darby NJ, Neuhaus D, Creighton TE. Two-dimensional 1H nuclear magnetic resonance study of the (5-55) single-disulphide folding intermediate of bovine pancreatic trypsin inhibitor. *J Mol Biol*. 1991. 222: 373-90.

Minnema M, Friederich F, Levi M, von dem Borne PAK, Mosnier L, Meijers J, Biemond J, Hack J,Bouma B, ten Cate H. Enhancement of rabbit jugular vein thrombolysis by neutralization of factor XI — in vivo evidence for a role of factor XI as an anti-fibrinolytic factor. *J Clin Invest*. 1998. 101: 10–14.

Mosnier LO, von dem Borne PK, Meijers J, Bouma BN. Plasma TAFI levels influence the clot lysis time in healthy individuals in the presence of an intact intrinsic pathway of coagulation. *Thromb Haemostasis.* 1998. 80: 829–835.

Mosnier LO, Meijers J, Bouma BN. Regulation of fibrinolysis in plasma by TAFI and protein C is dependent on the concentration of thrombomodulin. *Thromb Haemostasis*. 2001. 85: 5–11.

N

Nagashima M, Werner M, Wang M, Zhao L, Light D, Pagila R, Morser J, Verhallen P. An inhibitor of activated thrombin-activatable fibrinolysis inhibitor potentiates tissue-type plasminogen activator-induced thrombolysis in a rabbit jugular vein thrombolysis model. *Thromb Res*. 2000. 98: 333–342.

Narhi LO, Hua QX, Arakawa T, Fox GM, Tsai L, Rosenfeld R, Holst P, Miller JA, Weiss MA. Role of native disulfide bonds in the structure and activity of insulin-like growth factor 1: genetic models of protein-folding intermediates. *Biochemistry*. 1993. 32: 5214-21.

Neira JL, Itzahaki LS, Ladurner AG, Davis B, de Prat Gay, Fersh AR. Following cooperative formation of secondary and tertiary structure in a single protein molecule. 1997. *J Mol Biol.* 268: 185-197.

Neuhaus KL, von Essen R, Tebbe U, Jessel A, Heinrichs H, Maurer W, Doring W, Harmjanz D, Kotter V, Kalhammer E, et al. Safety observations from the pilot phase of the randomized r-Hirudin for Improvement of Thrombolysis (HIT-III) study. A study of the Arbeitsgemeinschaft Leitender Kardiologischer Krankenhausarzte (ALKK). *Circulation*. 1994. 90: 1638-42.

O

Oas TG, Kim PS. A peptide model of a protein folding intermediate. *Nature*. 1988. 336: 42-8.

Osterud B, Rapaport SI. Activation of factor IX by the reaction product of tissue factor and factor VII: additional pathway for initiating blood coagulation. *Proc Natl Acad Sci USA*. 1977. 74: 5260–5264.

P

Ptitsyn OB. Molten globule and protein folding. *Adv Protein Chem*. 1995. 47: 83-229.

R

Rand MD, Lock JB, Van't Veer C, Gaffney DP Mann KG. Blood clotting in minimally altered whole blood. *Blood*. 1996. 88: 3432–3445.

Rao KR, Brew K. Calcium regulates folding and disulfide-bond formation in alpha-lactalbumin. *Biochem Biophys Res Commun*. 1989. 163: 1390-6.

Redlitz R. Nicolini FA, Malycky JL, Topol EJ, Plow EF Inducible carboxypeptidase activity: a role in clot lysis in vivo. *Circulation*. 1996. 93: 1328–1330.

Rees DC, Lipscomb WN. Refined crystal structure of the potato inhibitor complex of carboxypeptidase A at 2.5 A resolution. *J Mol Biol*. 1982. 160: 475-98.

Refino CJ, DeGuzman L, Schmitt D, Smyth R, Jeet S, Lipari MT, Eaton DL. Bunting S. Consequences of inhibition of plasma carboxypeptidase B on in vivo thrombolysis, thrombosis and hemostasis. *Fibrinolysis Proteolysis*. 2000. 14: 305–314

Reverter D, Vendrell J, Canals F, Horstmann J, Aviles FX, Fritz H, Sommerhoff CP. A carboxypeptidase inhibitor from the medical leech Hirudo medicinalis. Isolation, sequence analysis, cDNA cloning, recombinant expression, and characterization. *J Biol Chem*. 1998. 273: 32927-33.

Reverter D, Fernandez-Catalan C, Baumgartner R, Pfander R, Huber R, Bode W, Vendrell J, Holak TA, Aviles FX. Structure of a novel leech carboxypeptidase inhibitor determined free in solution and in complex with human carboxypeptidase A2. *Nat Struct Biol*. 2000. 7: 322-8.

Rothwarf DM, Li YJ, Scheraga HA.Regeneration of bovine pancreatic ribonuclease A: detailed kinetic analysis of two independent folding pathways. *Biochemistry*. 1998. 37: 3767-76.

S

Sakata DJ, Loskutoff C, Gladson CL, Hekman CM, Griffin JH. Mechanism of protein C-dependent clot lysis: role of plasminogen activator inhibitor. *Blood*. 1986. 68: 1218–1223.

Schatteman KA, Goossens FJ, Scharpé SS, Hendriks DF. Activation of plasma procarboxypeptidase U in different mammalian species paints to a conserved pathway of inhibition of fibrinolysis. *Thromb Haemostasis*. 1999. 82: 1718–1721.

Schatteman KA, Goossens FJ, Scharpé SS, Hendriks DF. Proteolytic activation of purified human procarboxypeptidase U. *Clin Chim Acta*. 2000. 292: 25–40.

Scheraga HA, Konishi Y, Ooi T. Multiple pathways for regenerating ribonuclease A. *Adv Biophys*. 1984. 18: 21-41.

Scheraga HA, Wedemeyer WJ, Welker E. Bovine pancreatic ribonuclease A: oxidative and conformational folding studies. *Methods Enzymol*. 2001. 341: 189-221.

Sidelmann JJ, Gram J, Jespersen J, Kluft C. Fibrin clot formation and lysis: basic mechanisms. *Semin Thromb Hemost*. 2000. 26: 605-18.

Silveira A, Schatteman K, Goossens F, Moor E, Scharpe S, Strömqvist M, Hendriks D, Hamsten A. Plasma procarboxypeptidase U in men with symptomatic coronary artery disease. *Thromb Haemostasis*. 2000. 84: 364–368.

Skidgel RA. Human carboxypeptidase N: lysine carboxypeptidase. *Methods Enzymol*. 1995. 248: 653–663.

T

Takano S, Kimura S, Ohdama S, Aoki N. Plasma thrombomodulin in health and disease. *Blood*. 1990. 76: 2024–2029.

Tan AK, Eaton DL. Activation and characterization of procarboxypeptidase B from human plasma. *Biochemistry* 1995. 34: 5811–5816

Van Tilburg VH, Rosendaal FR, Bertina RM. Thrombin-activatable fibrinolysis inhibitor and the risk for deep vein thrombosis. *Blood*. 2000. 95: 2855–2859.

Thornton JM, Orengo CA, Todd AE, Pearl FM. Protein folds, functions and evolution. *J Mol Biol*. 1999. 293: 333-42.

U

Uversky VN, Ptitsyn OB. Further evidence on the equilibrium "pre-molten globule state": four-state guanidinium chloride-induced unfolding of carbonic anhydrase B at low temperature. *J Mol Biol*. 1996. 255: 215-28.

V

Valnickova Z, Thogersen IB, Christensen S, Chu CT, Pizzo SV, Enghild JV. Activated human plasma carboxypeptidase B is retained in the blood by binding to 2-macroglobulin and pregnancy zone protein. *J Biol Chem.* 1996. 271: 12937–12943.

Venhudova G, Canals F, Querol E, Aviles FX. Mutations in the N- and C-terminal tails of potato carboxypeptidase inhibitor influence its oxidative refolding process at the reshuffling stage. *J Biol Chem*. 2001. 276: 11683-90.

W

Wang W, Hendriks DF, Scharpé SS. Carboxypeptidase U, a plasma carboxypeptidase with high affinity for plasminogen. *J Biol Chem.* 1994. 269: 15937–15944.

Wedemeyer WJ, Welker E, Narayan M, Scheraga HA. Disulfide bonds and protein folding. *Biochemistry*. 2000. 39: 7032.

Weissman JS, Kim PS. Reexamination of the folding of BPTI: predominance of native intermediates. *Science*. 1991. 253: 1386-93.

Weissman JS, Kim PS. Kinetic role of nonnative species in the folding of bovine pancreatic trypsin inhibitor. *Proc Natl Acad Sci U S A*. 1992. 89: 9900-4.

Wu J, Yang Y, Watson JT. Trapping of intermediates during the refolding of recombinant human epidermal growth factor (hEGF) by cyanylation, and subsequent structural elucidation by mass spectrometry. *Protein Sci*. 1998. 7: 1017-28.

Wolynes PG, Onuchic JN, Thirumalai D. Navigating the folding routes. *Science*. 1995. 267: 1619-20.

Y

Yang Y, Wu J, Watson JT. Probing the Folding Pathways of Long R3 Insulin-like Growth Factor-I (LR3IGF-I) and IGF-I via Capture and Identification of Disulfide Intermediates by Cyanylation Methodology and Mass Spectrometry. *J Biol Chem*. 1999. 274: 37598-37604.

Z

Zhao L, Morser J, Bajzar L, Nesheim M Nagashima M, Identification and characterization of two thrombin-activatable fibrinolysis inhibitor isoforms. *Thromb Haemostasis*. 1998. 80: 949–955.

IX. APÉNDICE.

Material y métodos generales.

IX.A. REACTIVOS.

La termolisina (P-1512), el ditiotreitol (DTT), el glutatión reducido (GSH), el glutatión oxidado (GSSG), el β-mercaptoetanol y la trombina humana (10 NIH/ml) se obtuvieron de Sigma (St.Louis. Mo, USA) con grados de pureza mayores del 99%. La urea, el hidrocloruro de guanidinio (GdnHCl), el tiocianato de guanidinio (GdnSCN) y el acetonitrilo, con grados de pureza mayores al 99%, se obtuvieron de Merck (Darmstadt, Alemania).

El sustrato sintético de carboxipeptidasas hipuril-Arg y el inhibidor D-Phe-Pro-Arg clorometil cetona (PPACK) fueron obtenidos de Bachem (Bubendorf, Suiza). La trombomodulina de pulmón de conejo se obtuvo de American Diagnostica (Greenwich, CT). El activador de plasminógeno de tejidos recombinante (rt-PA) fue obtenido en forma comercial como Actilyse, alteplase, (145000 U/ml) fabricado por Boehringer Ingelheim (Ingelheim, Germany), como una aportación generosa del grupo de investigación en Hemostasia del Hospital de St.Pau (Barcelona).

IX.B. EXPRESIÓN HETERÓLOGA DEL LCI.

El LCI recombinante se ha obtenido mediante expresión heteróloga en la bacteria *E.Coli* siguiendo los procedimientos ya descritos que detallamos brevemente a continuación (Reverter, 1998). Para la producción recombinante de LCI, se inocularon 5 ml de la cepa de *E.Coli* MC1061 portadora de la construcción recombinante pIN-III-OmpA3-LCI y se crecieron O/N (*overnight*) a 37ºC en medio M9CAS (conteniendo 0.3% de glicerol). Este precultivo se utilizó para inocular 0.5 litros del mismo medio. Después del crecimiento durante dos horas, se añadió IPTG a una concentración final de 0.5mM. Tras 24 horas de su inducción el cultivo se centrifugó a 10000g durante 20 minutos, y el sobrenadante se aplica a un cartucho Sep-Pak Plus C18 (Waters, Millipore). El material unido se eluye con 30% de isopropanol y se concentra en un rotavapor para eliminar el solvente orgánico del eluído que contiene LCI.

Este extracto se disuelve en tampón Tris-acetato 20mM (pH 8), y se carga en una columna preparativa de intercambio aniónico (TSK-DEAE 5PW, 2.5 x 15 cm, Amersham Biosciences) conectada un sistema FPLC. La elución se llevó a cabo mediante un gradiente lineal de acetato amónico 0.8 M, en tampón Tris-acetato 20mM, del 0% al 100%, a un flujo de 4ml/min durante 80 minutos. La elución del LCI se obtiene al 60% de acetato amónico.

Las fracciones conteniendo el LCI se liofilizan y se someten a una posterior purificación por cromatografía de fase reversa-HPLC (columna Vydac C4) utilizando un gradiente lineal del 20% al 42% de acetonitrilo, en ácido trifluoroacético al 0.1%, a un flujo de 1ml/min durante 60 minutos. La proteína se obtiene de esta forma un 99% pura.

IX.C. DETERMINACIÓN DE LA MASA MOLECULAR DEL LCI RECOMBINANTE.

La masa molecular de la forma recombinante del LCI obtenido se analizó utilizando la técnica de espectrometría de masas, MALDI-TOF (*matrix assisted laser desorption/ionization-time-life-of-flight*). Los espectros de masas se adquirieron en un espectrómetro Bruker Biflex equipado con un láser de nitrógeno (337nm), en lineal o reflexión, modo ion positivo, y utilizando una aceleración de 19-kV de voltaje. Las matrices utilizadas para el análisis fueron el ácido sinapínico (ácido 3,5-dimetoxi-4-hidroxicinámico) o ácido α-ciano-4-hidroxicinámico. Las muestras se prepararon mezclando volúmenes iguales de una solución saturada de matriz en ácido trifluoroacético al 0.1% en agua/acetonitrilo 2:1. De esta mezcla, se toma 1 μl y se coloca en la muestra, ya depositada en la placa de espectrometría. A continuación se ha de permitir la evaporación hasta el secado de la muestra/matriz para posteriormente determinar el peso molecular.

IX.D. ESTUDIO DEL PLEGAMIENTO Y DESPLEGAMIENTO DEL LCI

IX.D.1. Experimentos de replegamiento oxidativo en ausencia de agentes redox (control + y control -).

Se toman 0.5 mg de LCI nativo, liofilizado, se reducen y desnaturalizan en tampón Tris-HCl (0.1M, pH 8.4) al que se ha añadido cloruro de guanidinio 6M y ditiotreitol 30mM. La reacción se lleva a cabo a 23ºC durante 90 minutos. Para eliminar el desnaturalizante y el reductor la muestra se purifica a través de una columna de gel-filtración NAP-5 (Amersham Biosciences), previamente equilibrada en tampón Tris-HCl (0.1M, pH 8.4) para permitir el inicio del replegamiento oxidativo. El LCI reducido y desnaturalizado recuperado se diluye

inmediatamente a una concentración final de 0.5mg/ml en el mismo tampón Tris-HCl, en dos condiciones: ausencia (control -) o presencia (control +) de β-mercaptoetanol 0.25mM. La reacción de replegamiento se detuvo a diversos tiempos previamente seleccionados (desde los 10 minutos hasta las 48 horas), mezclando alícuotas de la muestra con un volumen igual de ácido trifluoroacético al 4%. Los intermediarios atrapados en cada tiempo se analizaron mediante cromatografía de fase reversa-HPLC. Las condiciones de HPLC utilizadas fueron las siguientes. El solvente A es ácido trifluoroacético al 0.1% en agua, el solvente B es acetonitrilo/agua (9:1, v/v) conteniendo 0.085% de ácido trifluoroacético. La muestra se aplicó a una columna Zorbax 300SB C-18 (4.6mm x 5μm) y se desarrolló un gradiente linear entre el 31 y el 47% del solvente B en 45 minutos (zona donde se detectan todas las formas de la proteína entre el LCI nativo y el completamente desplegado) con un flujo de 0.5 ml/min a una temperatura de 23ºC.

IX.D.2. Plegamiento del LCI en presencia de agentes redox.

Los procedimientos de desplegado (reducción y desnaturalización) y el replegamiento se llevaron a cabo al igual que en el experimento de plegamiento control. Inmediatamente después de que el LCI desplegado fuera eluído de la columna de gel filtración NAP-5, al igual que en el experimento control, se diluyó a 0.5 mg/ml en tampón Tris-HCl al que se añadió GSSG (0.5mM) o una mezcla de GSSG/GSH (0.5mM/1mM). Se permite que la proteína se repliegue y se atrapan a los intermediarios de plegamiento mediante volúmenes iguales de ácido trifluoroacético al 4%. Las muestras se analizaron mediante cromatografía de fase reversa HPLC, en las mismas condiciones que los experimentos control.

IX.D.3. Desnaturalización y desplegamiento del LCI en presencia de un agente iniciador de la formación de tioles.

El LCI nativo (0.5 mg/ml) se disolvió en tampón Tris-HCl (0.1M, pH 8.4) al que se añadió β-mercaptoetanol 0.25 mM y una serie de concentraciones seleccionadas de agentes desnaturalizantes: Urea, de 0M a 8M, hidrocloruro de guanidinio de 0M a 8M, tiocianato de guanidinio de 0M a 6M, o solvente orgánico (metanol) del 35% al 65%. Se permitió que la reacción alcanzara el equilibrio manteniéndola durante 20 horas a 23ºC. Para monitorizar el efecto de los diversos agentes desnaturalizantes se tomaron alícuotas de las muestras tratadas, y la reacción fue detenida añadiendo un volumen igual al de la alícuota, de ácido trifluoroacético al 4%. Inmediatamente se analizaron mediante cromatografía HPLC o se guardaron a –20ºC hasta su análisis, excepto en el caso de las muestras desnaturalizadas por

tiocianato de guanidinio, que se purificaron, previamente a su análisis por HPLC, por gel-filtración (columnas NAP-5) y se eluyeron con ácido trifluoroacético al 1%, para retirar el GdmSCN. Para monitorizar las cinéticas de desplegamiento, el LCI nativo se disolvió en el mismo tampón Tris-HCl conteniendo hidrocloruro de guanidinio 6, 7 o 8M. A determinados tiempos tras la incubación, se extrayeron alícuotas, y se detuvo la reacción con un volumen igual de ácido trifuoroacético al 4%, para proceder así a su inmediato análisis por HPLC. La desnaturalización por calor se ensayó mediante la incubación de alícuotas de las muestras en tampón Tris-HCl (0.1M, pH 8.4) conteniendo β-mercaptoetanol 0.25mM a temperaturas crecientes (45ºC, 55ºC y 65ºC) durante una hora, y finalmente deteniendo el proceso con volúmenes iguales de ácido trifluoroacético al 4%. Todas los análisis por HPLC fueron realizados en las mismas condiciones que las cromatografías del experimento de replegamiento control.

IX.D.4. Análisis de los intermediarios de replegamiento oxidativo del LCI.

Los intermediarios capturados en medio ácido se fraccionaron por HPLC y se liofilizaron. Las muestras se derivatizaron con 50 μl de vinil-piridina 0.1M en tampón Tris-HCl (0.1M pH 8.4) a 23ºC durante 35 minutos y la reacción se detuvo mediante la adición de ácido trifluoroacético al 4%. Las muestras así derivatizadas se analizaron entonces mediante espectrometría de masas MALDI-TOF de cara a caracterizar el número de puentes disulfuro en la población de intermediarios de plegamiento, y a analizar los porcentajes de cada forma.

IX.D.5. Análisis estructural (identificación del apareamiento de cisteínas) de las trampas cinéticas III-A y III-B y de los isómeros *scrambleds* del LCI aislados del desplegamiento.

Las fracciones obtenidas por HPLC del los intermediarios III-A y III-B se aislaron, se congelaron y se derivatizaron con vinilpiridina tal y como se ha indicado en el apartado anterior. Las muestras derivatizadas con vinilpiridina se purificaron mediante HPLC y se congelaron. Los intermediarios aislados III-A1, III-A2, III-B y las fracciones aisladas del desplegamiento del LCI (20 μg de cada forma o intermediario) fueron tratados con 2μg de termolisina (Sigma, p-1512) en 30 μl de tampón N-etilmorfolin/acetato (50 mM, pH 6.4). Las digestiones fueron llevadas a cabo durante 16 horas a 37ºC, excepto para el caso de la especie X-LCI-a, que se realizó a 50ºC. Los productos termolíticos se aislaron mediante HPLC: se utilizaron las mismas condiciones que en el experimento de replegamiento control, excepto por el gradiente utilizado, que fue de 0 a 60% de solvente B, lineal, en 60 minutos. Los

péptidos de digestión purificados se analizaron mediante secuenciación de aminoácidos y espectrometría de masas MALDI-TOF a fin de identificar aquellos péptidos que contuvieran disulfuros.

IX.D.6. Secuenciación de aminoácidos y Espectrometría de Masas.

La secuencia de aminoácidos de los péptidos que contenían disulfuros se analizó mediante el método de Edman automatizado utilizando un secuenciador Procise, modelo 494 (PerkinElmer Life Sciences), equipado con analizador en línea de derivados de feniltiohidantoína. Las masas moleculares de los péptidos que contienen disulfuros se determinaron mediante espectrometría de masas MALDI-TOF (*matrix assisted laser desorption/ionization-time-life-of-flight*). En el caso de los péptidos de digestión de los intermediarios de replegamiento se utilizó un espectrómetro de masas Voyager-DE STR (Perkin Elmer Life Sciences) y en el caso de los péptidos de digestión de los isómeros *scrambled* del desplegamiento se utilizó un espectrómetro Bruker Bilfex TOF, equipado con un láser de nitrógeno con una longitud de onda de emisión de 337 nm.

IX.D.7. Espectrometría de fluorescencia del LCI tratado con Urea y con hidrocloruro de guanidinio.

El espectro de fluorescencia del LCI se midió con un espectrofluorómetro 650-40 *scanning* (Perkin-Elmer) de 300 a 450 nm, con excitación a una longitud de onda de 280 nm. El LCI fue disuelto en tampón Tris-HCl (1M pH 8.4) conteniendo β-mercaptoetanol 0.25 mM y concentraciones seleccionadas de desnaturalizantes (urea o hidrocloruro de guanidinio). La desnaturalización del LCI fue llevada a cabo a 23ºC durante 20 horas. La concentración final de LCI fue de 2 μM. Las intensidades de fluorescencia de las muestras blanco que contenían concentraciones equivalentes de desnaturalizante fueron asimismo analizadas y substraídas de las lecturas de las muestras con LCI.

IX.D.8. Trazado de las curvas de desnaturalización y desplegamiento del LCI.

La desnaturalización del LCI se define por la conversión de la estructura nativa a isómeros *scrambled*. La curva de desnaturalización se generó mediante el trazado del porcentaje de LCI nativo convertido a isómeros *scrambled* bajo concentraciones crecientes de un desnaturalizante seleccionado. En contraste, el desplegamiento describe el estado del LCI desnaturalizado y viene definido estructuralmente por la composición de los isómeros *scrambleds*. Las curvas de desplegamiento del LCI se determinan mediante las concentraciones

relativas de diferentes isómeros *scrambleds* existentes a lo largo del camino de desplegamiento bajo concentraciones crecientes de un desnaturalizante seleccionado. El cálculo de los isómeros *scrambled* se basó en la integración del área de los picos obtenidos. Los datos tienen una desviación estándart del $\pm$ 5%.

IX.E. EXPERIMENTOS DE FUNCIONALIDAD BIOLÓGICA DEL LCI

IX.E.1. Producción de proteínas recombinantes.

La producción a gran escala y la purificación del PCI y el LCI fue llevada a cabo tal y como ya se ha descrito brevemente en el primer subapartado del apéndice. Alícuotas de las proteínas obtenidas se liofilizaron y guardaron a –20ºC. Ambas proteínas se prepararon como soluciones concentradas de stock (1mg/ml) y se diluyeron en PBS (*fosfate buffer saline*) (NaCl 0.9%, PO_4HNa_2/PO_4H_2K 10mM, pH=7.2) justo antes de su uso.

IX.E.2. Preparación de las muestras de plasma.

El pool de plasma normal se obtuvo mediante la mezcla de plasmas de 50 voluntarios sanos. Las muestras de sangre se obtuvieron mediante venipunctura de la vena antecubital y fueron inmediatamente anticoaguladas mediante la adición de 1/10 del volumen de citrato sódico 0.129 M. Para obtener el plasma pobre en plaquetas las muestras de plasma se cenrtifugaron dos veces a 2500 x g durante 15 minutos. Las muestras de plasma se alicuotaron y se guardaron a –80ºC hasta su uso. Para obtener el suero inactivado se tomó el suero normalizado de 50 voluntarios sanos, se mezcló y se calentó a 56ºC durante 30 minutos, para provocar la pérdida de toda actividad carboxipeptidasa de base.

IX.E.3. Ensayo de fibrinólisis.

La lisis de los coágulos se estudió en un sistema de plasma en el cual la fibrinólisis mediada por t-PA de un coágulo inducido por trombina se mide por turbidimetría (Mosnier et al, 1998). Brevemente: el plasma citrado se diluye en PBS (1:4). Diversas concentraciones de los inhibidores (LCI o PCI) en un rango entre 30nM y 1μM se añaden al plasma diluído. En concreto, el plasma se incubó con las siguientes concentraciones seriadas de LCI: 0nM (control), 30nM, 50nM, 70nM, 90nM, 110nM; o bien se incubó con las siguientes

concentraciones de PCI 0nM (control), 30nM, 250nM, 500nM, 700nM, 1μM. Después del mezclado por agitación, 100 μl de esta mezcla se transfirieron inmediatamente al pocillo de una placa de microtitulación que contenía otros 100 μl de una solución de cloruro cálcico, t-PA, trombina y trombomodulina y se incubó a 37ºC. Las concentraciones finales de los reactivos son: cloruro cálcico 5.7 mM, t-PA 0.054 U/ml, trombina (1.1 IU/ml o 2.2 IU/ml) y trombomodulina (1.1 U/ml o 2.2 U/ml). En otra serie de ensayos no se añadió trombomodulina a las soluciones y la concentración de trombina se mantuvo igualmente a 1.1 IU/ml o 2.2 IU/ml. La absorbancia a 405 nm se siguió a 37ºC utilizando un lector de placas Anthos modelo A-5022 (Anthos labtec instruments, Salzburg) a intervalos de 30 minutos durante 6 horas. El tiempo de lisis de un coágulo se define como el tiempo que pasa entre la máxima turbidez y el punto medio de la transición de máxima turbidez a plasma transparente que caracteriza la lisis de la fibrina. Para cada punto de las curvas calculadas se representa la media de 5 experimentos independientes con 3 réplicas en cada experimento.

IX.E.4. Determinación de la actividad de TAFI en plasma.

La actividad de TAFI en plasma se determinó utilizando un método basado en la determinación colorimétrica del hipurato liberado por el enzima con un reactivo de cloruro de cianurilo/dioxano (Mosnier, 1998). Se determinó una curva estándart de la actividad de TAFI, para cada experimento, mediante diluciones seriadas de plasma normalizado en suero inactivado por calor, mientras que las muestras de plasma se determinaron por duplicado utilizando dos diluciones de plasma en suero inactivado (75% y 50% de plasma).

Puesto que la activación de TAFI depende de la cantidad de trombina y trombomodulina añadida al plasma (Bajzar, 1996), la actividad carboxipeptidasa determinada en plasma normal se llevó a cabo reproduciendo las concentraciones de trombina y trombomodulina empleadas para activar TAFI en el ensayo de lisis de coágulos (1.12 IU/ml o 2.2 IU/ml, concentraciones finales). Para iniciar la activación de TAFI, se añadió trombina, trombomodulina y cloruro cálcico (17mM) a 30 μl de plasma normalizado sin ningún inhibidor o con LCI (110 nM) o PCI (500 nM), y el volumen se ajustó a 60 μl con tampón HEPES 20mM (N- [2.hidroximetil] – piperazine-N' [ácido 2-etanelsulfónico], pH 7.4) que contenía cloruro sódico 150 mM y cloruro cálcico 5mM. Tras 10 minutos de incubación a temperatura ambiente la activación de TAFI se paró por la adición de PPACK (D-Phe-Pro-Arg clorometil cetona) (20μl, 20μM) y después de la mezcla la conversión a ácido hipúrico se permitió durante 10 minutos. La reacción del sustrato se detuvo mediante la adición de 20 μl de ácido clorhídrico 1M seguido

por la adición de igual volumen de hidróxido sódico 1M. Se añadieron 25 μl ml de fosfato sódico 1M (pH 7.4) a cada muestra para satisfacer los requerimientos de fosfato de la determinación colorimétrica de hipurato mediante cloruro de cianurilo/dioxano. Finalmente se añadieron 60 μl de cloruro de cianurilo al 3% disueltos en dioxano y se permitió que se desarrollara el color mediante un mezclado vigoroso. La mezcla de incubación se centrifugó a 14000 rpm durante 2 minutos en una microcentrífuga Eppendorf para extraer la proteína desnaturalizada y el exceso de cianúrico y se tranfirieron 100 μl de cada muestra a una placa de microtitulación. La absorbancia se midió a 405 nm en un lector de microplacas Anthos (Anthos labtec intruments, Salzburg).

Para distinguir entre la actividad carboxipeptidasa constitutiva (CPN) y la actividad carboxipeptidasa inducible (TAFIa) en el plasma, la actividad de TAFIa se calculó como la actividad carboxipeptidasa sensible a la inhibición por concentraciones saturantes de PCI (25 μg/ml) (Sakharov et al, 1997). La actividad carboxipeptidasa que permanece a concentraciones saturantes de PCI es lo que se toma como actividad CPN constitutiva y se sustrae de la actividad carboxipeptidasa total obtenida en cada muestra. Las actividades de TAFI en las muestras de plasma se expresaron como un porcentaje de la concentración de TAFIa en plasma normal.

IX.E.5. Microscopía electrónica de rastreo (SEM).

Los coágulos se examinaron durante la fase rápida del ensamblaje de la fibrina y la fibrinólisis cuando se pueden observar diferencias profundas entre la turbidez de los coágulos sin inhibidor y los coágulos tratados con LCI o PCI. Para iniciar la activación de TAFI y la coagulación se utilizaron concentraciones de 2.2 U/ml de trombina y trombomodulina. Se seleccionaron seis puntos, a lo largo del tiempo, de la curva de fibrinólisis para su análisis por microscopía de rastreo. Micromuestras de los coágulos de plasma se colocan en una placa cubierta de parafilm, se lavan abundantemente con PBS y se tratan inmediatamente con el fijador primario (2% de glutaraldehído en 0.1M de PBS, pH 7.4) a determinados tiempos. Después de la fijación en tetróxido de osmio al 1% en PBS durante 90 minutos, se deshidratan mediante concentraciones crecientes de acetona y se desecan por desecado en punto crítico. Las muestras desecadas se sombrean de manera rotacional con oro y las micrografías subsecuentes de las áreas representativas se observaron en un microscopio electrónico de rastreo Hitachi s-570 (Hitachi LT. Tokyo, Japan). Cada figura posee una magnificación correspondiente a la escala que se indica por la barra que se muestra en la base de las micrografías y representa una distancia de 5 μm. El grosor de la fibras de fibrina se analizó a

partir de las micrografías utilizando el programa para el procesado de imágenes Metamorph, Version 4.6r5 (Universal Imaging corporation).

IX.E.6. Microscopía electrónica de transmisión (TEM).

Micromuestras de coágulos de plasma (preparadas y seleccionadas tal y como acabamos de describir) se aplicaron a rejillas de carbono y se tiñeron negativamente con uranilo de acetato al 2%. Las imágenes se tomaron en un microscopio electrónico JEOL 1200EX-II operado a 100kV y fueron grabadas en una película Kodak SO-163 a una magnificación nominal de 60000 aumentos.